



ASHESI UNIVERSITY

**DESIGN AND FABRICATION OF A SOLAR POWERED
STIRLING ENGINE AS A WATER PUMPING MACHINE**

CAPSTONE

B.Sc. Mechanical Engineering

Theodora Mamle Mate-Kole

2020

ASHESI UNIVERSITY

DESIGN AND FABRICATION OF A SOLAR POWERED STIRLING ENGINE AS A WATER PUMPING MACHINE

CAPSTONE PROJECT

Capstone Project submitted to the Department of Engineering, Ashesi University in partial fulfilment of the requirements for the award of Bachelor of Science degree in Mechanical Engineering.


Theodora Mamle Mate-Kole

2020

DECLARATION

I hereby declare that this capstone is the result of my own original work and that no part of it has been presented for another degree in this university or elsewhere.

Candidate's Signature:


.....

Candidate's Name:

Theodora Mamle Mate-Kole
.....

Date:

29th May, 2020.
.....

I hereby declare that the preparation and presentation of this capstone were supervised in accordance with the guidelines on supervision of capstone laid down by Ashesi University College.

Supervisor's Signature:

.....

Supervisor's Name:

.....

Date:

.....

Acknowledgements

I would like to thank God for guiding me throughout this project. I am most grateful to my supervisor Dr. Kenobi Morris for his guidance and support at every point of this project. To Joseph Timpabi and Peter Lawerh Kwao for their time and effort put into this project to make sure it was a success. Their dedication is deeply appreciated. I would also like to thank my family, who catered to my every whim and my friends who constantly encouraged me.

Abstract

As the world keeps evolving, the demand for electricity increases. The growing energy consumption leads to higher cost that many people, especially in Ghanaian rural areas, cannot afford. Thus, considering this, this paper focuses on designing a Stirling engine to pump water in homes. In order to contribute to the use of renewable energy with a low carbon footprint, concentrated solar energy will be used to power this system once it is implemented. As such this, source of power was considered in the design of the Stirling engine. The Stirling engine was designed in Solidworks. Simulations were also done in Solidworks and MATLAB to test the performance of the designed engine. Using the Schmidt formula, the work and power output of the engine was calculated.

Table of Content

Acknowledgements	III
Abstract	IV
Table of Figures	VII
1 Introduction	1
1.1 Problem Statement	1
1.2 Project Objectives	2
1.3 Theoretical or Conceptual Framework.....	3
1.3.1 The First Law of Thermodynamics.....	3
1.3.2 Heat Exchangers	3
1.3.3 Schmidt Analysis	3
2 Literature Review.....	4
2.1 History	4
2.2 Types of Stirling Engines.....	4
2.3 Operation of the Stirling Engine	7
2.4 Solar Powered Systems	8
2.4.1 Systems that Produce Electricity	9
2.4.2 Systems for Water Pumping Purposes.....	11
3 Design Requirements and Criteria	16
3.1 Design Proposal.....	16
3.2 Requirements.....	17
3.2.1 User Requirements.....	17
3.2.2 System Requirements.....	17
3.3 Design Criteria and Decision Matrix	18
3.3.1 Working Fluid.....	18
3.3.2 Stirling Engine Configuration.....	19
3.4 Material Selection	20
3.5 Selecting Hot and Cold Side Temperatures	22
4 Design and Implementation	23
4.1 Analysis and Calculations	23
4.1.1 Power Analysis	24
4.1.2 Analysis of Flywheel	26
4.1.3 Heat Exchanger Analysis.....	26
4.1.4 Fin Analysis	29
4.1.5 Slider Crank Mechanism.....	31

4.2	Dimensions of the Various Parts of the Engine	32
4.3	Fabricated Prototype	32
5	Results and Discussion	36
5.1	Simulations.....	36
5.1.1	Thermal Analysis of Cooling Fins.....	36
5.1.2	Stress and Fatigue Analysis of Crankshaft	37
5.1.3	Stress and Fatigue Analysis of Displacer.....	38
5.1.4	Stress and Fatigue Analysis of Power Piston.....	39
5.2	Thermodynamic Analysis	41
6	Conclusion	42
6.1	Limitations	42
6.2	Future Work	43
	References	44
	Appendix.....	48
	Appendix A: Modelled and Fabricated Stirling Engine	48
	Appendix B: Schmidt Analysis.....	50
	Nomenclature for Analysis	50
	Assumptions to perform Schmidt Analysis [7], [25]	51
	Schmidt Analysis [7], [26].....	51
	Appendix C: Drawings of the Parts of the Stirling Engine.....	54

Table of Figures

Figure 2.1: Alpha Stirling engine.....	6
Figure 2.2: Beta Stirling engine	6
Figure 2.3: Gamma Stirling engine.....	6
Figure 2.4: P-V diagram of the Stirling cycle [11]	8
Figure 2.5: An assembly of Roelf J. Meijer's Design	8
Figure 2.6: Schematic of the proposed system by Mike He and Seth Sanders [13]	10
Figure 2.7: Model of designed solar Stirling engine [15]	11
Figure 2.8 : Sunpulse Water Pump Connected to a Borehole [16]	12
Figure 2.9: 3D model of Anish Saini, Shivam Kohli and Ajesh J. Pillai's Stirling engine and pump [17]	13
Figure 3.1: Block diagram of the system	16
Figure 3.2: Thermal Conductivity against Price	21
Figure 3.3: A graph the densities of Various Metals	21
Figure 4.1: Typical Water Pump used in Households	25
Figure 4.2: Annular Cooling Fins [6]	30
Figure 4.3: Diagram showing the slider crank mechanism.....	31
Figure 4.4: The basic structure of the gamma Stirling engine [7]	32
Figure 4.5: Displacer.....	33
Figure 4.6: Power piston	34
Figure 5.1: Simulation results of cooling fins.....	36
Figure 5.2: Stress analysis of crankshaft.....	37
Figure 5.3: Fatigue analysis of crankshaft	38
Figure 5.4: Results of the displacer's fatigue analysis	39
Figure 5.5: Results of the displacer's static analysis	39
Figure 5.6: Results of power piston's fatigue analysis.....	40
Figure 5.7: Results of power piston's static analysis	40
Figure 5.8: PV diagram of Stirling engine.....	41
Figure A1 : A top view of designed Stirling engine	48
Figure A2: Aside view of designed Stirling Engine	48

Figure A4: Top view of the prototype built	49
Figure A3: Front view of the prototype built.....	49
Figure C1: Drawing of Displacer Cylinder.....	54
Figure C2: Drawing of Power Cylinder.....	55
Figure C3: Drawing of Power Piston.....	56
Figure C4: Drawing of Connecting Rod.....	57
Figure C5: Drawing of Flywheel	58
Figure C6: Drawing of Crankshaft	59
Figure C7: Drawing of Crankshaft Support.....	60
Figure C8: Drawing of the Displacer Cylinder's Support.....	61
Figure C9: Drawing of Power Cylinder's Support.....	62
Figure C10: Drawing of Displacer Cylinder.....	63
Figure C11: Drawing of Connecting Tube	64
Figure C12: Drawing of the base of the Engine	65
Figure C13: Exploded View of Stirling Engine.....	66

1 Introduction

1.1 Problem Statement

Electricity is one of the significant determinants of the prosperity of a country's economic. It plays a substantial role in our daily activities such as heating, cooking, and communicating. As such, electricity is crucial for human existence. However, not every human enjoys the privileges that come with electricity. As of 2017, only 79% of the population had access to electric power in Ghana [1], while 43% of the entire African population has access to electricity [2]. This makes performing daily activities such as pumping water for domestic use challenging, especially in rural areas and farms. Water is also a fundamental human need since it is used to perform many activities such as cooking, bathing and irrigation of plants. As such, there is always a high demand for water in these communities. However, due to the limited supply of electricity, the pumping or channeling of water to the various homes for use is nearly impossible.

A simple solution to this problem may be to expand the energy grid of the country to cover these areas. However, this comes at a cost that most people in rural areas cannot afford. Moreover, most of the energy utilized is usually produced by diesel, gas or coal, which are non-renewable sources of fuel, hence, may run out soon. These sources of energy also cause much pollution in the environment. For instance, for each gallon of gasoline used, 8.7 kg of carbon dioxide is emitted, while 12.2 kg is emitted for 1 gallon of diesel used [3]. Though expanding the energy grid to these rural areas is a potential solution to mitigate the existing challenges, nevertheless, the rural community could hardly bear the cost that comes with such solutions. Thus, the need for an alternative solution that is relatively cheaper and sustainable with little or no harm to the environment. Considering these conditions, a better alternative may be the use of renewable energy

such as solar energy. Solar energy is a clean and free source of power that can be harnessed either using photovoltaic cells or a solar thermal collector for power generation on large scales. Similarly, this concept can be altered and used solely for water pumping in rural areas without electricity, with the use of a solar collector and a Stirling engine.

1.2 Project Objectives

This project seeks to design a purely mechanical water pump driven by a Stirling engine. Stirling engines have the versatility of being able to be powered by any heat source. However, this project seeks to emphasize the importance of renewable energy, specifically, solar energy. As such, a solar collector will be used to harness the sun's energy to power the Stirling engine. The Stirling engine is a critical section of the system, and hence, it is the focus of this project.

It must be noted that people in rural areas are mostly below the poverty bracket. The World Bank defines poverty as individuals who cannot afford \$1.9 per day [4]. As such, the fundamental design goal is to achieve high efficiency at low cost. In order to reduce the initial and maintenance cost of the system, local resources will be outsourced. This project aims to fulfil one of the goals of the Sustainable Development Goal (SDG) 7, to ensure access to affordable, reliable, sustainable and modern energy for all. SDG 7 seeks to “increase substantially the share of renewable energy in the global energy mix” [5].

The main project objectives are listed below:

- Designing a low-cost Stirling engine for water pumping.
- Making use of renewable sources of energy that is, Concentrated Solar Power to design the engine.

1.3 Theoretical or Conceptual Framework

1.3.1 The First Law of Thermodynamics

A Stirling Engine is a thermodynamic cycle that consists of thermodynamic processes such as the transfer of heat, and the production work. Thermodynamic cycles are governed by the first law of the thermodynamics, which states that energy can neither be created nor destroyed, but changes from one form to the other [6]. The first law allows for the transformation of heat into other energy sources such as electrical and mechanical energy by employing a power cycle. Power cycles are the underlying principle behind the operation of heat engines. In this project, the power cycle of an internal combustion cycle is studied and utilized.

1.3.2 Heat Exchangers

Heat exchangers are devices used in the transfer of heat between two or more fluids at different temperatures. Unlike mixing chambers, fluids involved in the heat exchange are not allowed to be mixed [6]. In order for this system to work efficiently, a heat exchanger is employed to facilitate the transfer of heat to and from the environment.

1.3.3 Schmidt Analysis

Schmidt Analysis is one of the fundamental theories used in the design of the Stirling engine. It is used in calculating the isothermal processes associated with the Stirling cycle [7]. Schmidt analysis is useful in predicting the power output of the Stirling engine, and it is utilized in predicting the work done and power output of the designed Stirling engine.

2 Literature Review

2.1 History

Robert Stirling, a minister in the Church of Scotland, produced the first-ever Stirling engine on September 27, 1816. At the time, the engine was known as the hot air engine. Similar to the modern Stirling engines, Robert Stirling's engine worked based on the cyclic heating and cooling of an internal gas such as air, hydrogen and helium. The name, Stirling engine was later devised by Roelf Meijer, a Dutch engineer to describe similar engines known as a closed cycle regenerative gas engine [8].

However, Robert Stirling's engine was hardly used in the 1990s due to the invention of more powerful internal combustion such as the steam engine. This was because the Stirling engine was bound to fail when its hot cylinder was heated beyond its capacity [8]. Nevertheless, its quiet operation enable it to be used in submarines as a source of power [8].

2.2 Types of Stirling Engines

A Stirling engine is a heat engine that operates by the compression and expansion of air or other gases known as a working fluid such that there is a conversion of thermal energy into mechanical energy. It is a closed cycle, meaning that the working fluid used is permanently contained in the system and does not need to be renewed as in other cycles such as the Rankine cycle [9]. It is environmentally harmless and silent in its operation. Stirling engines can operate using several gases such as hydrogen, nitrogen, helium and the most common being air. Theoretically, the efficiency of such engines is about 52% to 72% [10]. There are three main types of Stirling engines which are distinguished by the way they are constructed and how the working

fluid moves from the cold region to the hot area. These are the Alpha, Beta and Gamma Configurations.

The Alpha Stirling engine in Figure 2.1 consist of two pistons in two separate cylinders, that is, the hot piston and the cold piston which is connected by a tube containing the regenerator. Both cylinders, which are 90 degrees apart, are connected to a flywheel at a common point. Due to the reciprocal motion of both pistons, the working fluid is repeatedly moved back and forth from the cold cylinder to the hot cylinder. As a result, the working fluid is heated and cooled in every cycle. This causes the working fluid to expand upon heating and contract when cooled in the cold cylinder. The expansion and contraction of the working fluid forces the piston to move linearly, which provides power for the rotational movement of the flywheel.

Unlike the alpha Stirling engine that has two power pistons, the beta Stirling engine has one cylinder containing, the power piston and the displacer. As the name suggests, the power piston is used to produce the power required for the engine to operate while the displacer's function is to move the working fluid back and forth from the heated region to the cold area. When the working fluid moves into the hot zone, it expands and pushes the power piston up, and the flywheel is turned. In the cold zone, the working fluid contracts and the momentum of the flywheel pushes the power piston down to compress the fluid. A typical beta engine is shown in Figure 2.2.

Gamma Stirling engines are similar to beta Stirling engines; however, the power piston is found in a separate cylinder as in Figure 2.3. Both pistons are however connected to the same flywheel with the displacer 90 degrees ahead of the power piston. The Gamma Stirling engine has large dead volumes as compared to the Alpha and Beta Stirling engines since there is an introduction of a passageway to connect the displacer and the power piston [8]. However, this type of engine is mechanically simpler, and therefore, it is the preferred engine used.

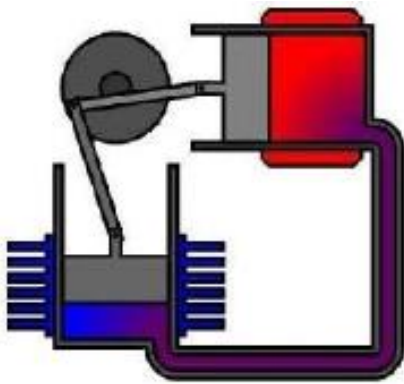


Figure 2.1: Alpha Stirling engine

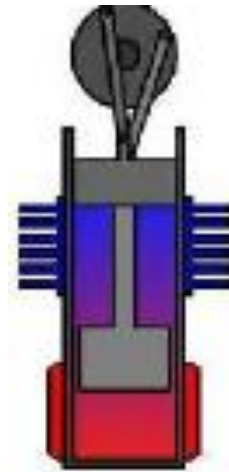


Figure 2.2: Beta Stirling engine

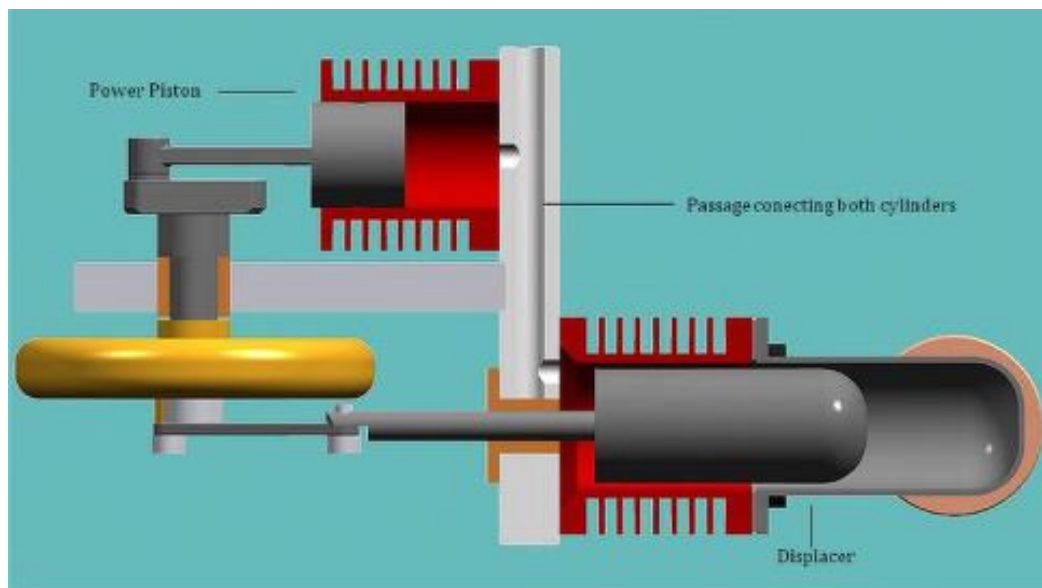


Figure 2.3: Gamma Stirling engine

2.3 Operation of the Stirling Engine

The Stirling cycle is based on four thermodynamic processes explained as follows, and it is summarized in the P-V diagram in Figure 2.4:

- **Isothermal expansion (1):** In this stage, the heated fluid in the hot region expands and pushes the power piston outward to turn the flywheel.
- **Constant volume heat removal (2):** The gas is transferred from the hot region to the cold zone. Before it gets to the cold area, the gas passes through the regenerator where heat is removed stored for use in the next cycle. In the cold region, heat is lost at constant volume.
- **Isothermal compression (3):** The momentum of the flywheel pushes the piston inwards, which forces the working fluid to compress, thereby, reducing its volume. As this is being done, heat is removed from the engine to the environment. The gas is also transferred from the cold region to the hot area.
- **Constant volume heat addition process (4):** The working fluid is found in the heated region at this point. Heat is added at constant volume. In cases where there is a regenerator, heat is added to the working fluid as it transferred from the cold region to the heated region.

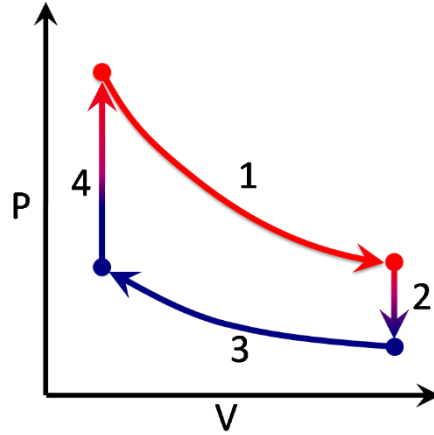


Figure 2.4: P-V diagram of the Stirling cycle [11]

2.4 Solar Powered Systems

Due to the intense research into renewable energy specifically, solar energy, to cater for the emission of greenhouse gases by non-renewable energy, the Stirling engine technology was revived. The solar-powered Stirling engines were first patented by Roelf J. Meijer in 1987 [11]. His design, shown in Figure 2.5, consisted of a large dish with a focal point at the centre of the dish where the sun's energy was concentrated. The concentrated heat then powers the Stirling engine, which is used to produce electricity. After Roelf J. Meijer patented his work, many similar systems were studied and also constructed for the production of electricity.

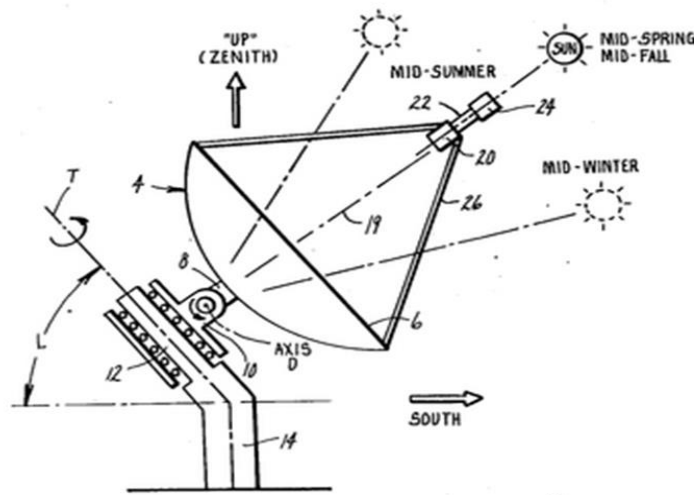


Figure 2.5: An assembly of Roelf J. Meijer's Design

Ranjani Vasu and Firas Basim Ismail cover various literature on solar-powered Stirling engine. The development and the types of Stirling engines (i.e. Beta, gamma and alpha Stirling engines) are discussed as well. The paper examines the factors that affect Stirling engine performance which gives insight as to how an all-rounded solar Stirling engine can be developed for future studies. Some of the factors that affect the performance of the engine include the mass and size of the engine. A micro-sized Stirling engine which weighs 10g and has a swept volume of 0.05 cm^3 was able to produce an output power of 10mW at a frequency of 10 Hz. The heat conductivity between the reservoir and the engine is also a significant factor affecting the engine's performance [12]. In a nutshell, the main conclusions arrived at are as follows:

- The Stirling engine has a simple working principle, uses an external heat source, has high efficiency as compared to other heat engines, and it has a low cost of operation.
- The highest possible efficiency can be achieved by setting up a double-acting piston arrangement in the gamma configuration.
- The working fluid used must have:
 - Low viscosity
 - High specific heat capacity
 - High thermal conductivity

2.4.1 Systems that Produce Electricity

Mike He and Seth Sanders [13] addressed the challenges associated with the generation of electricity, such as an economically appealing system by proposing a low-temperature differential Stirling engine-based system for the production of electricity. A low-temperature differential

(LTD) Stirling engine is an engine which operates with a temperature difference between 100°C and below. LTD engines usually have a relatively large surface area to facilitate the transfer of heat between the environment and the engine [14]. He and Sander's [13] proposed system in Figure 2.6 encompasses a passive solar thermal collector, a thermal energy storage system, a Stirling engine and a waste heat recovery system for a combined heat and power system. The Stirling engine is the significant component of the system; as such, the authors' primary focus in this paper. The major design goal described are ways in which the heat engine can be designed to attain high enough efficiency at low cost and low hot-side temperature. As such, the low cost of materials and fabrication of a low-temperature differential system is of primary concern. In order to achieve relatively high efficiency, the focus was on designing an economical and efficient heat exchanger by minimizing temperature drops along the path of the thermal energy. After evaluations and testing, the engine selected was a gamma type Stirling engine with an operating frequency of 20 Hz at a pressurized air, at 30 Bar, as the working fluid.

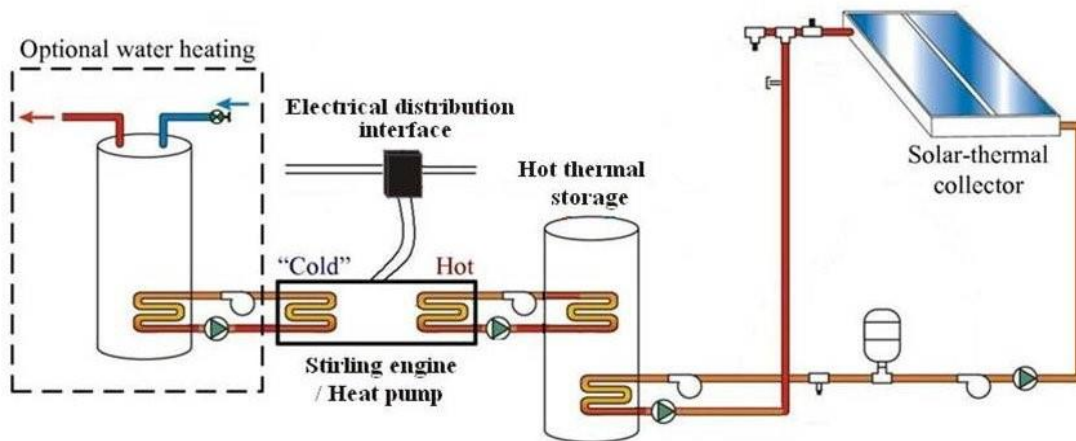


Figure 2.6: Schematic of the proposed system by Mike He and Seth Sanders [13]

Aditya, A et al. [15] emphasized the use of a solar Stirling engine for power generation with a focus on the parabolic reflector as a heat source for the engine in their paper. Based on calculations, the engine designed is that of a gamma- configuration, double-acting vertical Stirling engine. This system consists of a parabolic reflector with a convex lens, a Stirling engine and a tacho generator to convert mechanical energy to electrical energy. The modelling of the different parts of the system shown in Figure 2.7 was done using Solid edge. The efficiency of the engine designed based on calculations was 71.8% which is higher than other internal combustion engines [15].

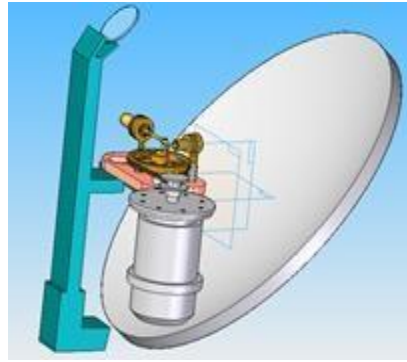


Figure 2.7: Model of designed solar Stirling engine [15]

2.4.2 Systems for Water Pumping Purposes

Other than the production of electricity, solar-powered Stirling engines can be used for other applications which require mechanical energy. A typical example of such an application is the pumping of water, which is the main focus of this paper. In this section, systems that are solely used for water pumping activities will be discussed and reviewed.

A solar thermal water pump was recently designed and fabricated by Sunvention Sunpulse Water (Figure 2.8). It consists of a solar thermal collector, a Stirling engine which is coupled to a water pump. The advantage of this system is that it can be coupled to any mechanical device which requires similar power to that of the water pump. The system was specifically designed using

locally available non-toxic and recyclable materials. According to the World Bank, the existing “maximum water cost target” is 6 US cents/m³. Currently, gasoline pumps cost 8.58 US cents/m³ while photovoltaic systems are estimated at 8.5 US cents/m³. The Sunvention Sunpulse water pump is assessed to cost 2.4 US cents/m³, which is 60% below the World Bank’s set target [16]. Hence, we can conclude that solar-powered Stirling engines are a good alternative for other pumping systems as it is relatively cheaper.

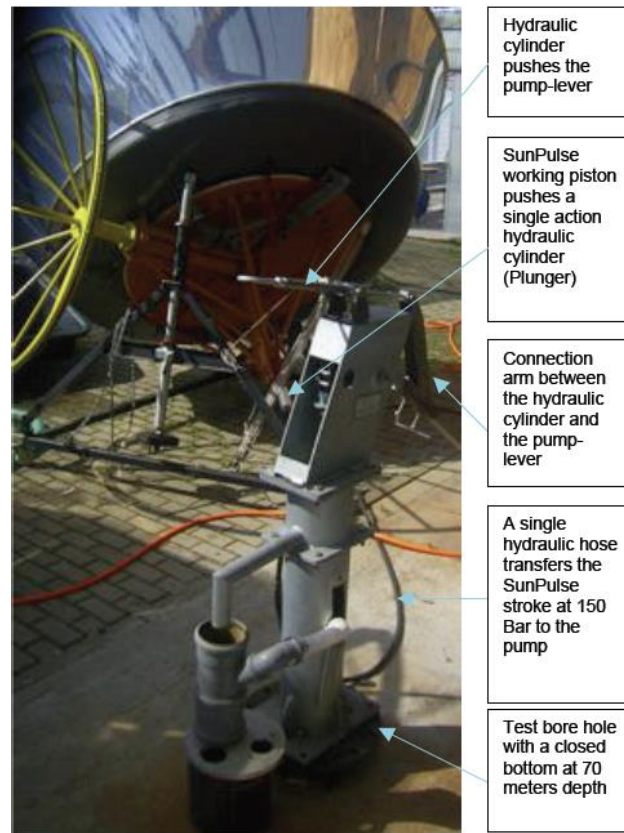


Figure 2.8 : Sunpulse Water Pump Connected to a Borehole [16]

Anish Saini, Shivam Kohli and Ajesh J. Pillai [17] write on the use of solar energy to power a water pump with the help of a Stirling engine to capture the sun’s thermal energy. To concentrate the solar beams into a specific area for the Stirling engine, a parabolic mirror is used. From Anish Saini, Shivam Kohli and Ajesh J. Pillai’s design in Figure 2.9, they estimated an output approximately 3kW, which can drive a centrifugal pump at a speed of 500-1,500 rpm. In cases of lower power output, a gear mechanism can be used to achieve the desired speed or torque. For the

system to begin operation, an initial momentum must be given to the flywheel of the engine. According to these authors, once a temperature of about 500⁰C is achieved by the concentrated solar collector, the displacer piston moves forward, thereby forcing the power piston to move. The force of the power piston is transferred to the flywheel, which acts as an energy reservoir. The flywheel then transfers its rotary motion to the centrifugal pump which is connected to the same shaft (In this system, there is no gear mechanism). The design parameters of Anish Saini, Shivam Kohli and Ajesh J. Pillai's system are summarized in Table 2.1. The authors argue that this system of pumping water is the most efficient and economical since no electricity is being utilized, and it has low maintenance cost as well as little operational cost [17].

Table 2.1: Design parameters of Anish Saini, Shivam Kohli and Ajesh J. Pillai's Stirling engine and pump [17]

• Engine Type	• 2 Piston
• Main Energy Source	• Solar Energy
• Working Fluid	• Helium
• Mean Pressure	• 3-6 MPa
• Max. Expansion Space Temp.	• 975⁺₋₅₀ K
• Max. Shaft Power	• 3KW
• Engine Speed	• 500-1500 rpm
• Output Mechanism Type	• 60 deg. V Crank
• Flywheel Inertia	• 0.9 Kg m

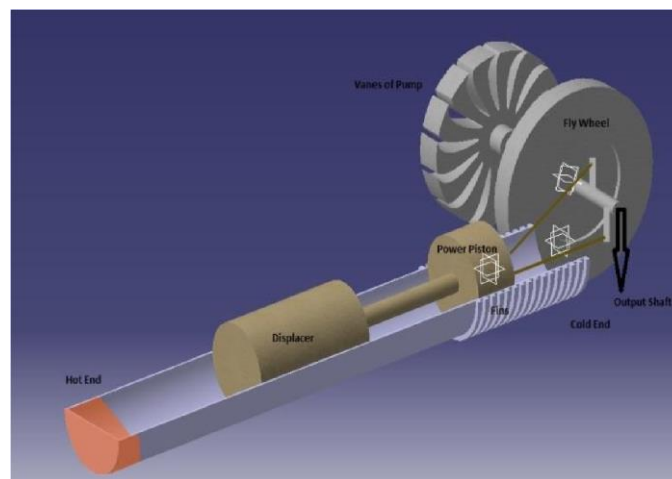


Figure 2.9: 3D model of Anish Saini, Shivam Kohli and Ajesh J. Pillai's Stirling engine and pump [17]

A review was also done on the different types of systems (including photovoltaic cell systems) that use Stirling engines for water pumping. The paper relates the evaluation of solar Stirling engines to several factors namely,

- (1) Areas where underground water is available and needed
- (2) The daily volume of water to be pumped
- (3) The pumping depth
- (4) Site features and climatic conditions
- (5) Infrastructure and local technical skills
- (6) Technical alternatives available for water pumping

The authors state that the electrical power needed to drive a working pump is calculated based on equation 2.2 [18]. The power obtained determines the amount of power the Stirling engine needs to power a water pump:

$$W = \frac{\rho g V H}{3600} = 0.002725 \left(\frac{Wh}{day} \right) \quad (2.1)$$

The paper concludes that a gamma Stirling engine can be developed to pump water. Air is usually used as a working fluid in such systems due to the difficulty of obtaining other working fluids. The operation of the engine is based on the speed of the centrifugal pump attached. The temperature ranges for such an engine can be designed to be between 70⁰C and 800⁰C with an efficiency between 52% and 72% [18].

Based on the studies above, the following conclusions about the Stirling engine can be made:

- The gamma type Stirling engine is the most widely used, as it is easy to construct since the power piston and displacer piston are a certain distance apart, unlike the beta Stirling engine where both pistons are aligned.
- Solar-powered Stirling engines are environmentally friendly and have little to no carbon footprint as compared to photovoltaic (PV) panels [19].
- As compared to other systems, the solar-powered Stirling engine is relatively cheaper and has a less operational cost, as stated in M. Ardon's report [16].
- The Stirling engine can work using various heat sources once there is adequate temperature. Hence, it can be operated as a hybrid system. However, since the focus of this paper is to promote the use of renewable energy, solar energy will be the primary source of heat for the Stirling engine.
- The ideal temperature difference required for the effective operation of a low-temperature differential Stirling engine is between 100⁰C [14].

3 Design Requirements and Criteria

This chapter establishes the desired user requirements, technical specifications, as well as the entire proposed system. Based on the user and system requirements obtained from secondary research, various design considerations, including material selection, selecting the right dimensions and configuration will be introduced to achieve the desired goal.

3.1 Design Proposal

The objective of this project is to build a prototype of a heat engine, that is, a Stirling engine to pump water mainly for rural areas such as the Accra in Ghana, which records a temperature of 32°C on an average. To achieve this, the Stirling engine, with its calculated dimensions, was designed and simulated in Solidworks. After which the prototype was fabricated. The functional block diagram of the system is shown in Figure 3.1.

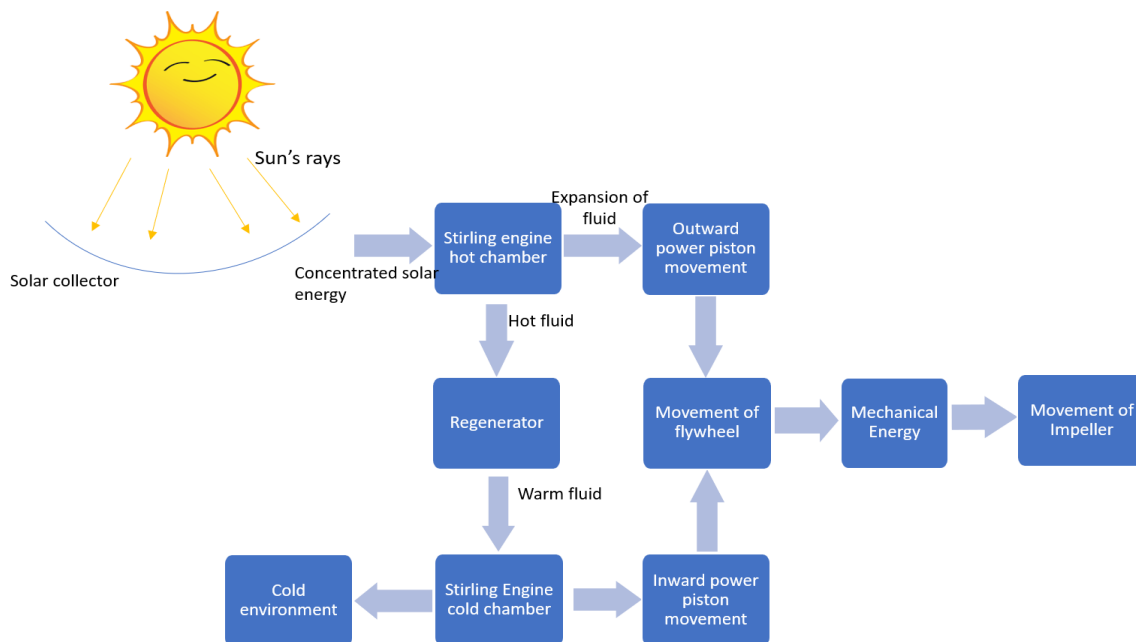


Figure 3.1: Block diagram of the system

3.2 Requirements

The requirements outlined include requirements from the user's perspective, as well as the system requirements based on its functionalities. These requirements were obtained mainly through literature reviews and user interviews. With the help of these requirements listed, the system was designed according to the user's preferences. The users of this system include people living in sunny rural areas in Ghana and homeowners. The user requirements and system requirements are listed in section 3.2.1 and 3.2.2, respectively.

3.2.1 User Requirements

- The system should be cost-effective
- The system should be easy to maintain (Simple system)
- The system should be able to last long enough
- Should be able to pump water fast enough and silently

3.2.2 System Requirements

- The system should be able to drive the water pump efficiently with a high flow rate
- The system (Stirling engine) should be able to work with any heat source
- The system should be simple
- The system should be environmentally friendly (low carbon footprint)

3.3 Design Criteria and Decision Matrix

In order to achieve the goals of this system, a design criterion was set, and a decision matrix was created to evaluate specific aspects of the system. A Pugh matrix was constructed for the various working fluids and the three Stirling engine configurations.

3.3.1 Working Fluid

Common working fluids used in the operation of the Stirling engine include hydrogen, air, helium, and nitrogen. These working fluids are evaluated and assigned scores based on the criteria found in Table 3.1. The various criteria include density, viscosity, thermal diffusivity, specific heat capacity, safety, availability, and cost of the fluid. The criteria were weighted based on its importance and the requirements of the project. Density deals with how heavy the fluid is. For this system, very light gas is desired for the smooth operation of the engine. Viscosity describes the internal friction of the fluid. For the easy flow of the fluid, a low viscosity is required. Thermal diffusivity involves the transfer of heat from one particle of the fluid to the adjacent particle. Specific heat capacity is also concerned with the amount of heat required to raise the temperature of 1 kg of the fluid by 1⁰C. For an optimal system, high thermal diffusivity and low specific heat capacity are desired. Among all the other working fluids, air had the highest rating. Therefore, it would be used in the operation of the system being designed.

Table 3.1: Pugh Matrix of the Working Fluids [6]

Design Criterion	Weight	Hydrogen		Air		Helium		Nitrogen	
		Score	Rating	Score	Rating	Score	Rating	Score	Rating
Density	0.1	5	0.5	2.5	0.25	4	0.4	1	0.1
Viscosity	0.15	4	0.6	2	0.3	1	0.15	3	0.45
Thermal Diffusivity	0.1	4.5	0.45	3	0.3	4	0.4	2	0.2
Specific Heat Capacity	0.1	5	0.5	1.5	0.15	3	0.3	0.5	0.05
Safety	0.2	3	0.6	5	1	1	0.2	1	0.2
Availability	0.15	3	0.45	5	0.75	2	0.3	4	0.6
Cost	0.2	0.5	0.1	5	1	2	0.4	4	0.8
Total			3.2		3.75		2.15		2.4

3.3.2 Stirling Engine Configuration

The main types of configurations of a Stirling engine are the alpha, beta and gamma configurations. These configurations are explained in detailed in section 2.2. The various criteria used in the configuration selection include the manufacturability, sealing, low dead volume and its operation at low differentials. Manufacturability considers how easy and affordable it is to design and machine the system. Sealing deals with how the working fluid can be trapped in the engine without escaping. Dead volume is the total volume in a Stirling engine (either in the hot or cold space) that is not being swept by the pistons. An increase in the dead volume causes a decrease in the efficiency of the engine. Therefore, a low dead volume is required for optimization [20]. An engine with low-temperature differential is desired due to the nature of the environment the system will be located. The weight for each criterion is assigned based on its importance. Table 3.2 lists the various criteria, and the configurations are scored according to how well they perform in each section. Overall, the gamma type Stirling engine scored the highest. As such, the system being built will be based on the gamma Stirling engine design.

Table 3.2: Pugh Matrix for Stirling Engine Configurations

Design Criterion	Weight	Alpha		Beta		Gamma	
		Score	Rating	Score	Rating	Score	Rating
Manufacturability	0.5	2	1	1	0.5	4	2
Sealing	0.2	1	0.2	4	0.8	3	0.6
Low Dead volume	0.15	4	0.6	4	0.6	2	0.3
Operation at low temperature differentials	0.15	2	0.3	3	0.45	5	0.75
Total	1		2.1		2.35		3.65

3.4 Material Selection

The project aims to create a relatively low-cost water pumping system. Therefore, the material selected should be affordable and locally outsourced. The materials under consideration include light metals with high thermal conductivity. The CES EduPack software aided in the material selection process. The criteria used in selecting the material was the thermal conductivity of the material, the cost, and the density of the material. The thermal conductivity of the suitable metals is graphed against its price in Figure 3.2. The most suitable metals obtained from this graph are aluminum and copper alloys which has a thermal conductivity of 121 W/m⁰C -137 W/m⁰C and 50 W/m⁰C - 300 W/m⁰C, respectively. The densities of these materials graphed in Figure 3.3 are 2640 kg/m³-2810 kg/m³ and 8180 kg/m³ – 8850 kg/m³, respectively. Due to the relatively high density of copper, aluminum alloy would be used for the fabrication of the main parts of the engine such as the displacer, power piston and the cooling fins.

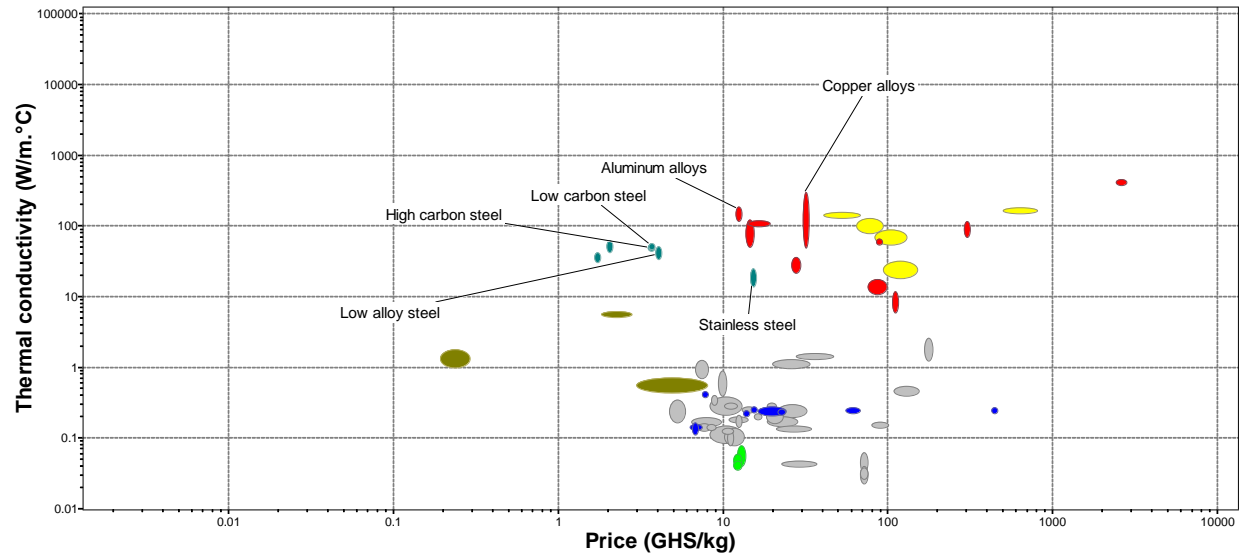


Figure 3.2: Thermal Conductivity against Price

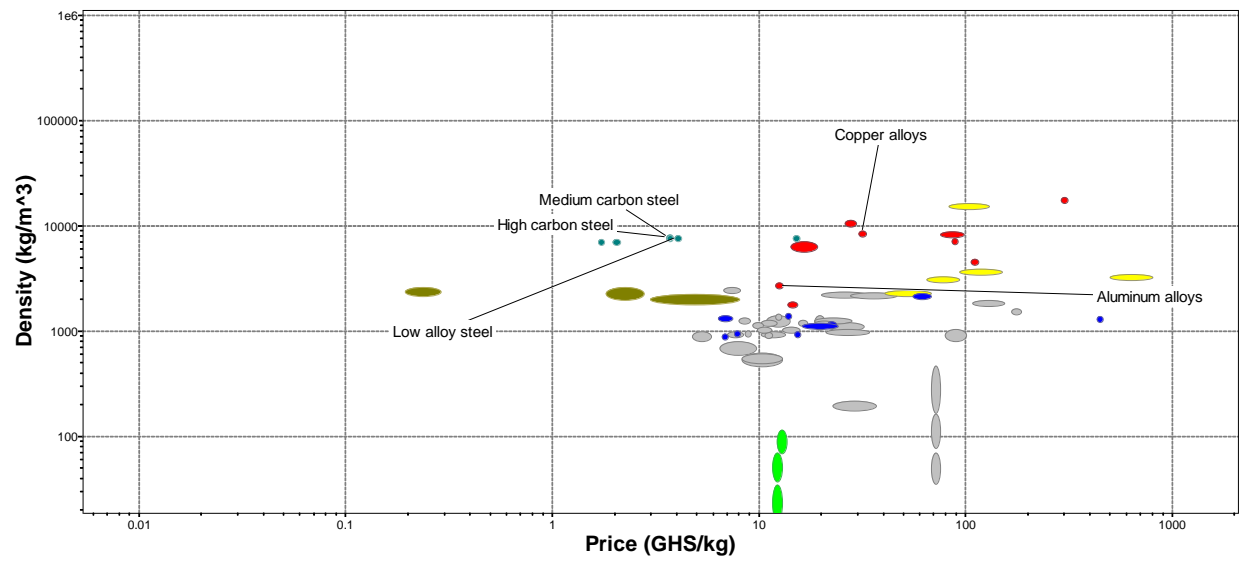


Figure 3.3: A graph the densities of Various Metals

3.5 Selecting Hot and Cold Side Temperatures

As stated above, ideally, the system would be powered by a solar parabolic dish collector. As such, the Stirling engine was designed such that it works based on the temperature produced by the solar collector. The expected temperature range produced by a small-sized solar collector is between 150°C–300°C [21]. Therefore, the hot side was designed based on this temperature. While the hot side is at a temperature, T_h of 300°C, the cold side was designed to be at temperature, T_c of 200°C to achieve a temperature difference of 100°C [14].

4 Design and Implementation

Chapter 4 describes the various processes and calculations involved in obtaining the precise dimensions for the system to be modelled using Solidworks.

4.1 Analysis and Calculations

Table 4.1 contains all the variables and its definitions used in this chapter.

Table 4.1: Table of Variables

Variable	Definition and unit
A_S	Area of displacer cylinder, m ²
$A_{fin\ area}$	Surface area of cylinder with fins, m ²
A_{fin}	Area of a fin, m ²
D_{disp}	Diameter of displacer cylinder, m
L_{dis}	Length of displacer cylinder, m
$L_{fin\ area}$	Length of the cylinder with fins, m
L_{fin}	r1-r2, m
L_c	Length of the piston connecting rod, m
Q_{fin}	Heat transfer of surface with fins, W
Q_{nofin}	Heat transfer of surface without fins, W
$Q_{supplied}$	Heat supplied to the Stirling Engine, W/
T_h	Temperature at hot side, °C
T_{avg}	Average temperature of cylinder, °C
T_b	Bulk mean temperature, (Tb+Tinf)/2, °C
T_c	Temperature at cold side, °C
T_f	Film temperature, °C
T_{inf}	Ambient temperature, °C
$m_{flywheel}$	Mass of flywheel, kg
r_1	Inner radius of a fin, m
r_2	Outer radius of a fin, m
r_{crank}	Radius of crankshaft, m
$r_{flywheel}$	Radius of flywheel, m
S_{opt}	Optimum spacing of fins, m

t_{fin}	Thickness of a fin, m
$t_{flywheel}$	Thickness of flywheel, m
v_{pis}	Velocity of piston, m/s
ε_{fin}	Fin effectiveness
η_{carnot}	Carnot efficiency of Stirling engine
ρ_{al}	Density of Aluminum, kg/m ³
ω_{rad}	Angular velocity in rad/s
ω_{rpm}	Angular velocity in rpm
F	Friction factor
g	Acceleration due to gravity
h	convection heat transfer coefficient, W/m ² ·°C
I	Moment of Inertia
k	Thermal Conductivity
Nu	Nusselt number
Pr	Prandtl number
Ra	Rayleigh's number
Re	Reynold's number
U	Overall coefficient of heat transfer, W/m ² K
ν	Kinematic viscosity, m ² /s
X	Distance moved by piston, m
α	Thermal diffusivity, m ² /s
β	Volume expansion coefficient, 1/K
η	Pump efficiency
V	Volume of flywheel, m ³
θ	Crank angle, °

4.1.1 Power Analysis

In order to obtain the required power to drive the water pump efficiently, the Stirling engine's dimensions were obtained based on the power required. As such, the following calculations were done to obtain the required power for modelling the engine.

Using a typical household water pump shown in Figure 4.1, the following data in Table 4.2 was obtained:



Figure 4.1: Typical Water Pump used in Households

Table 4.2: Ratings of a Typical Water Pump

Ratings	Value
Flowrate, Q_{\max}	$0.00055 \frac{\text{m}^3}{\text{sec}}$
Energy Head, H_{\max}	33 m
Power, P_{pump}	370 W
Power, P_{\max}	550 W
η	67.27%

From the ratings of the pump, the power needed to drive it is 370W. This is equivalent to the power to be supplied by the Stirling engine. However, due to the inefficiencies of the Stirling engine, the power produced would be less than expected. Therefore, the actual power produced by the Stirling was calculated using its Carnot efficiency in equation 4.1 [6].

$$\eta_{\text{carnot}} = 1 - \frac{T_c}{T_h} \quad (4.1)$$

The Carnot efficiency achieved was 33.3%. Therefore, to account for inefficiencies of the system, the actual power that the engine is expected to produce, Q_{stirling} is 1.11 kW which was

calculated using equation 4.2. This power obtained is equivalent to the heat energy produced by the Stirling engine [6].

$$Q_{stirling} = \frac{P_{pump}}{\eta_{carnot}} \quad (4.2)$$

4.1.2 Analysis of Flywheel

The dimensions of the flywheel were calculated based on the desired energy required and its moment of inertia using equations 4.3 to 4.8 [22]. A radius of 0.2568 m was obtained for the flywheel assuming an engine speed of 1200 rpm [23].

$$Kinetic\ Energy\ per\ cycle, E = \frac{P \times 60}{\omega} \quad (4.3)$$

$$Moment\ of\ Inertia, I = \frac{2 \cdot E}{\omega_{rpm}^2 \cdot 60} \quad (4.4)$$

$$I = \frac{1}{2} \cdot m_{flywheel} \cdot r_{flywheel}^2 \quad (4.5)$$

$$But\ m_{flywheel} = \rho_{al} \cdot V \quad (4.6)$$

$$and\ V = \pi r_{flywheel}^2 t_{flywheel} \quad (4.7)$$

$$\therefore I = \frac{1}{2} \cdot P_{al} \cdot \pi \cdot r_{flywheel}^4 \cdot t_{flywheel} \quad (4.8)$$

4.1.3 Heat Exchanger Analysis

To model the heat exchanger effectively, using the desired hot region and cold region temperatures obtained from literature, the log mean temperature difference (LMTD) must be implemented. The LMTD method is an effective method for obtaining the dimensions of the heat exchanger. Once the log mean temperature difference, ΔT_{lm} , the overall heat transfer coefficient, the mass flowrates and the heat required are known, the area of the heat exchanger, as well as its length, can be calculated for, using equations 4.29 and 4.30. This heat exchanger is modelled as a

parallel heat exchanger. That is, both working fluid and ambient air all move in the same direction.

The equations governing parallel-flow heat exchanges are equations 4.9 to 4.11.

$$\Delta T_1 = T_h - T_{inf} \quad (4.9)$$

$$\Delta T_2 = T_c - T_{inf} \quad (4.10)$$

$$\Delta T_{lm} = \frac{\Delta T_1 - \Delta T_2}{\log \left(\frac{\Delta T_1}{\Delta T_2} \right)} \quad (4.11)$$

Given that:

$$T_{inf} = 32 \text{ }^\circ\text{C}$$

$$T_h = 300 \text{ }^\circ\text{C}$$

$$T_c = T_h - 100 \text{ }^\circ\text{C}$$

ΔT_{lm} can be calculated for as 214.1222.

Next, to find the overall heat transfer coefficient in equation 4.28, h_1 and h_2 , which represents the convective coefficient for the ambient air and the working fluid, respectively, need to be calculated. h_1 , which can be classified as natural convection, can be obtained from equations (4.17 to 4.21 [6]. To use these equations, certain properties of the air need to be estimated using the film temperature in equation 4.12. These properties, that is, the Prandtl number, the thermal conductivity, kinematic viscosity and volume expansion coefficient, are shown in equations 4.13 and 4.16 using a film temperature of 166°C (439 K) [6].

$$T_f = \frac{T_{h1} + T_{inf}}{2} + 273 \text{ K} \quad (4.12)$$

$$Pr_1 = 0.7007 \quad (4.13)$$

$$k_1 = 0.0355 \text{ W/m} \cdot \text{K} \quad (4.14)$$

$$v_1 = 3.0461 \times 10^{-5} \text{ m}^2/\text{s} \quad (4.15)$$

$$\beta_1 = \frac{1}{T_f} \text{ K}^{-1} \quad (4.16)$$

$$Ra = \frac{g\beta(T_s - T_{inf})L^3}{v^2} Pr \quad (4.17)$$

$$\text{Where } T_s = T_{h1} + 273 \quad (4.18)$$

$$\text{and } T_{inf} = T_c + 273 \quad (4.19)$$

$$Nu = \left\{ 0.6 + \frac{0.387Ra^{\frac{1}{6}}}{\left[1 + \left(\frac{0.559}{Pr} \right)^{\frac{9}{16}} \right]^{\frac{8}{27}}} \right\}^2 \quad (4.20)$$

$$h = \frac{k \cdot Nu}{D_{disp}} \quad (4.21)$$

To find h_2 , the flow of the working fluid in the cylinder is considered as forced convection. As such, equations 4.25 to 4.27 and 4.21 were used to find the value of h_2 as 46.1348 W/m²K. The properties of air used to find h_2 at a film temperature of 450 °C (723 K), are in expressions 4.22 to 4.24. After finding both coefficients of convections, the overall coefficient of heat transfer U, can be found using equation 4.28. The area and length of the heat exchanger, that is, the displacer cylinder, is then calculated in equation 4.29 and 4.30 respectively.

$$Pr_2 = 0.6946 \quad (4.22)$$

$$k_2 = 0.04104 \text{ W/m} \cdot \text{K} \quad (4.23)$$

$$v_2 = 4.091 \times 10^{-5} \text{ m}^2/\text{s} \quad (4.24)$$

$$Re = \frac{v_{pis} \cdot D_{disp}}{v^2} \quad (4.25)$$

$$f = (0.790 \ln Re - 1.64)^{-2} \quad (4.26)$$

$$Nu = \frac{\left(\frac{f}{8}\right) (Re - 1000) Pr}{1 + 12.7 \left(\frac{f}{8}\right)^{0.5} \left(Pr^{\frac{2}{3}} - 1\right)} \quad (4.27)$$

$$\frac{1}{U} = \frac{1}{h_1} + \frac{1}{h_2} \quad (4.28)$$

$$A_s = \frac{Q}{U \cdot \Delta T_{lm}} \quad (4.29)$$

$$L_{dis} = \frac{A_s}{\pi \times D_{dis}} \quad (4.30)$$

4.1.4 Fin Analysis

Cooling fins are projections on the surface of heat exchangers to increase the surface area and hence, radiate heat away from a device. The annular cooling fins in Figure 4.2 is incorporated in the design of the Stirling engine's heat exchanger is to optimize the rate of heat transfer at the cold region. To justify the added material and cost associated with the cooling fins, the performance of the fins is expressed in terms of fin effectiveness, ε_{fin} . The fin effectiveness is defined as in equation 4.31. For the fins to enhance heat transfer effectively, the effectiveness of the fins should be greater than one ($\varepsilon_{fin} > 1$) [6]. As such the finned surface was designed around this effectiveness to obtain the right dimensions for optimal heat transfer. Equations 4.32 to 4.39 are used to obtain the cooling fins dimensions in Table 4.3 [6]:

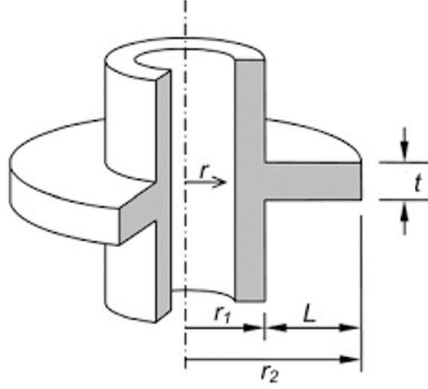


Figure 4.2: Annular Cooling Fins [6]

$$\varepsilon_{fin} = \frac{Q_{fin}}{Q_{nofin}} \quad (4.31)$$

$$Q_{fin} = \varepsilon_{fin} \cdot Q_{nofin} \quad (4.32)$$

$$\text{Where } Q_{nofin} = h \cdot A_{fin \text{ area}} \cdot (T_b - T_{inf}) \quad (4.33)$$

$$\text{and } A_{fin \text{ area}} = \pi \cdot D \cdot L_{fin \text{ area}} \quad (4.34)$$

$$\text{Area of fin, } A_{fin} = \frac{Q_{fin}}{h(T_b - T_{inf})} \quad (4.35)$$

$$r_2 = r_{2c} - \frac{t}{2} \quad (4.36)$$

$$\text{Where } r_{2c} = \sqrt{\frac{A_{fin}}{2\pi} + r_1^2} \quad (4.37)$$

$$\therefore D_2 = r_2 \times 2 \quad (4.38)$$

$$L_{fin} = r_2 - r_1 \quad (4.39)$$

The cooling fins must be spaced out in such a manner to transfer heat out of the system effectively.

The optimum spacing, 0.0095 m, is derived using the equation 4.40 below [24].

$$s_{opt} = 2.71 \times \left(\frac{g\beta(T_b - T_{inf})}{L\alpha v} \right)^{-\frac{1}{4}} \quad (4.40)$$

4.1.5 Slider Crank Mechanism

The slider-crank mechanism is a critical part of the Stirling engine because it converts the linear motion of the piston to the rotary motion needed by the impeller of the water pump. Figure 3.1 simplifies the slider-crank mechanism of the crankshaft and the piston. The connecting rod, l_c connects the piston to the crankshaft which has a radius, r_{crank} . Equations 4.41 and 4.42 govern the working principle of the mechanism.

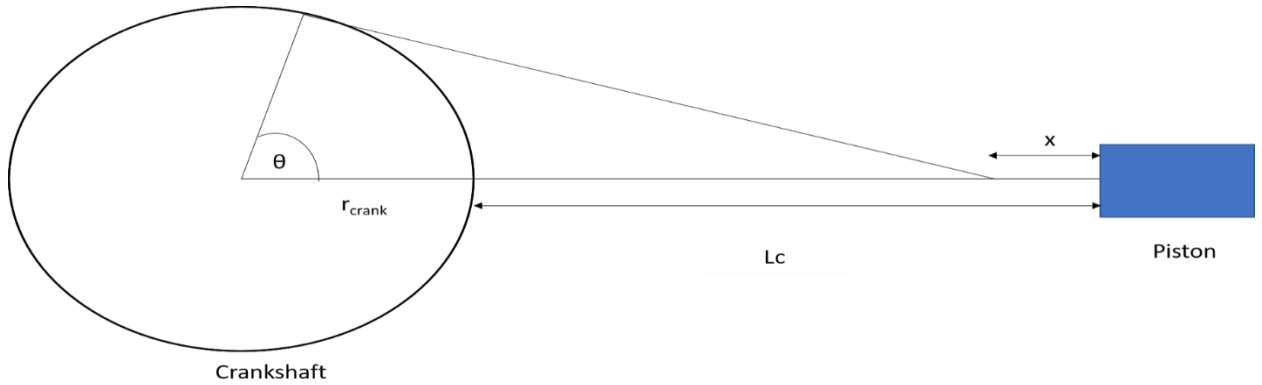


Figure 4.3: Diagram showing the slider crank mechanism

$$x = r_{crank} \left(1 - \cos \theta + \frac{K^2}{2} \sin^2 \theta \right) \quad (4.41)$$

$$\text{Where } K = \frac{r_{crank}}{l_c} = 0.3 \quad (4.42)$$

From the dimensions obtained, the maximum distance travelled by the displacer, is 0.098 m hence, making the crankshaft turn an angle of 180° . With this angle, θ and the distance travelled by the displacer, equations 4.41 and 4.42 [22] are manipulated to obtain the crankshaft radius, r_{crank} as 0.0489 m.

4.2 Dimensions of the Various Parts of the Engine

The dimensions of the other parts of the engines were acquired from Figure 4.4, which shows the basic structure of the Stirling engine.

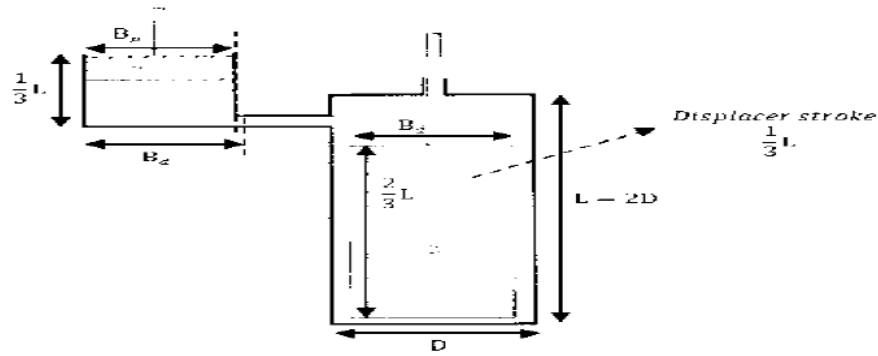


Figure 4.4: The basic structure of the gamma Stirling engine [7]

Table 4.3: Dimensions of the Main Parts of the Stirling Engine

Engine Part	Dimension (m)
Displacer Cylinder	Outer diameter: 0.365
	Inner diameter: 0.362
	Length: 0.744
Displacer	Diameter: 0.355
	Length: 0.496
Power Cylinder	Outer diameter: 0.180
	Inner diameter: 0.177
	Length: 0.297
Power Piston	Outer diameter: 0.177
	Length: 0.248
Cooling Fins	Thickness: 0.005
	Diameter: 0.699
	Optimum spacing: 0.0095
Flywheel	Thickness: 0.015
	Diameter: 0.514

4.3 Fabricated Prototype

With the dimensions in Table 4.3, the Stirling engine was modelled, as shown in Appendix A:

Modelled and Fabricated Stirling Engine

Using a scale of 1:13 of the dimensions in Table 4.3, a prototype was built. Figure A43 and Figure A34 show a picture of the prototype built. Since the prototype was built to test out the functionality of the system, it was built using common materials such as an aluminum cans, steel rods and aluminum plate. The following steps describe how each of the parts was built:

1. An aluminum can was cut to the desired length to function as the displacer cylinder.
2. The displacer was fashioned from foam with a thin steel rod in the middle to act as the connecting rod as shown in Figure 4.5 .



Figure 4.5: Displacer

3. The power cylinder was fashioned from a 22mm PVC pipe elbow. One end of the pipe elbow was attached to the side of can. To make the attachment easier, the pipe elbow was shaped to match the curve of the can using sandpaper. Once that was done, the curved end of the pipe elbow is attached the side of the aluminum can using epoxy.
4. A hole is made at the side of the can where the pipe elbow is attached. This will aid in the movement of air to and from the power cylinder.
5. A balloon is used to cover the free end of the pipe elbow. This will help in moving the power piston.

6. To cover the displacer cylinder, a second identical aluminum can is cut to length and placed over the free end of the displacer cylinder with the displacer inside. A hole is made in the top can, to facilitate the movement of the displacer's connecting rods. The cylinder is sealed with epoxy to make it airtight.
7. Two plastic sticks are attached to the displacer as shown in figure A4. A 2mm hole is made at the top of the plastic sticks. The holes made on both sticks should be aligned horizontally. This will support the crankshaft.
8. A steel rod of diameter 2 mm was obtained to serve as a crankshaft. Since the displacer is always 90° ahead of the power piston, the crankshaft was bent such that the movement of the pistons satisfy this rule. The fabricated crankshaft was passed through the holes of the sticks as shown in figures A3 and A4.
9. The displacer was connected to the crankshaft by wrapping its connecting rod to the crankshaft.
10. The power piston was fabricated from a 1mm steel rod. The steel rod was coiled at one end and attached to the balloon using epoxy as shown in Figure 4.6. The other end was wrapped around the crankshaft.



Figure 4.6: Power piston

11. A CD was attached to the free end of the crankshaft to function as the flywheel.

To provide energy for the fabricated engine, a candle was used. The estimated temperature of the heat provided was 85°C. Coldwater at an estimated temperature of 15°C was placed in the top can. This provides the needed temperature difference needed to run the engine. A speed of 123 rpm was obtained from the working engine. The estimated power output of the engine was 0.28 W. The low power output can be attributed to the low quality of materials used and the small temperature difference. The optimum temperature difference needed from the effective working of the engine is 100°C [14]. Once the size of the engine is scaled up to the required dimensions, using the appropriate materials and optimum temperature difference, the desired power can be achieved.

5 Results and Discussion

This chapter discusses the various simulations and analysis done to ensure the proper working of the system once it is implemented physically.

5.1 Simulations

After modelling the engine in Solidworks, the critical parts of the engine were simulated.

5.1.1 Thermal Analysis of Cooling Fins

With the dimensions obtained from the calculations in chapter 5, the cooling fins were modelled and simulated to test the amount of heat it can dissipate out of the system. A temperature of 300°C was set on the inside of the fins while a convective coefficient was set around the body. With a fin of diameter 0.699 m, the temperature difference it could achieve was 160°C, as shown in Figure 5.1. This temperature difference is high enough to optimize the working of the engine.

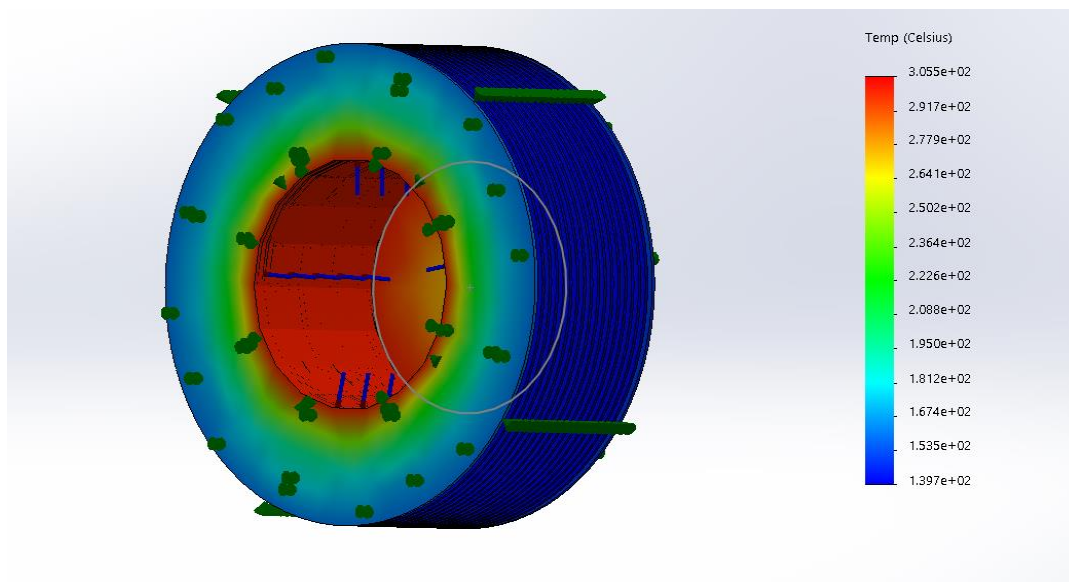


Figure 5.1: Simulation results of cooling fins

5.1.2 Stress and Fatigue Analysis of Crankshaft

The crankshaft, which is made out of steel (as typical crankshafts are made from steel), with a diameter 15 mm was analyzed to determine the stresses that it will face when the engine is in operation. The crankshaft is analyzed with all supports and forces acting on it, as shown in Figure 5.2. The maximum stress occurs on one of the fixtures with a value of $5.663 \times 10^7 \text{N/m}^2$. The yield stress for this material is $2.750 \times 10^8 \text{N/m}^2$. Therefore, the maximum stress experienced is significantly below the yield stress. Hence the minimum factor of safety is 4.9. As such, this crankshaft is suitable for its operation. Figure 5.3 shows the results obtained from the fatigue analysis. The analysis shows that, after 1,000,000 cycles, there will be a damage percentage of 6.58 %.

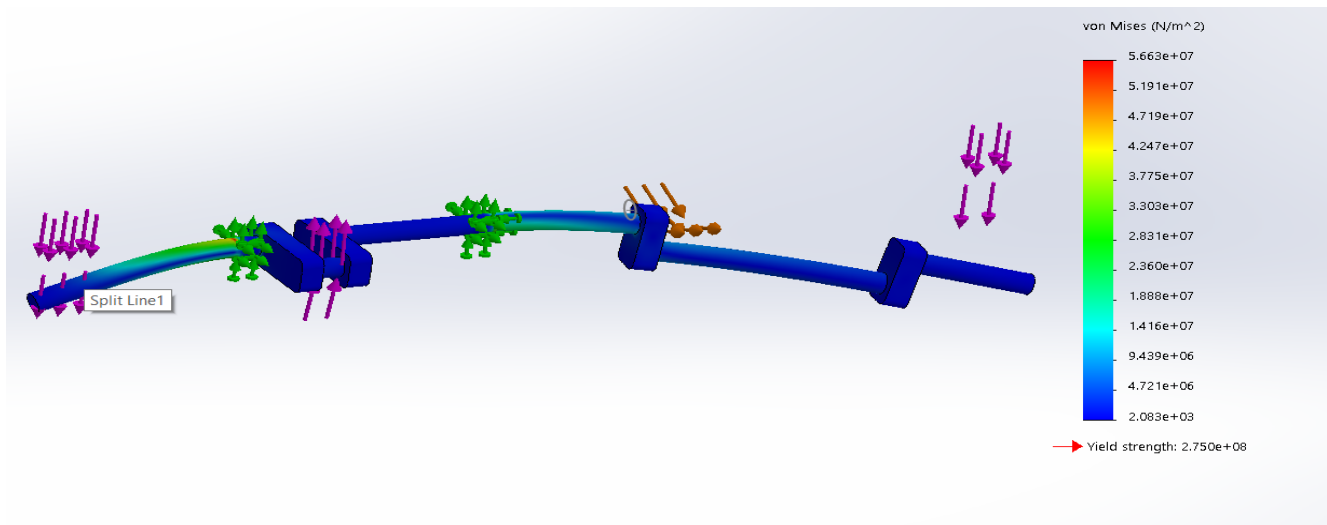


Figure 5.2: Stress analysis of crankshaft

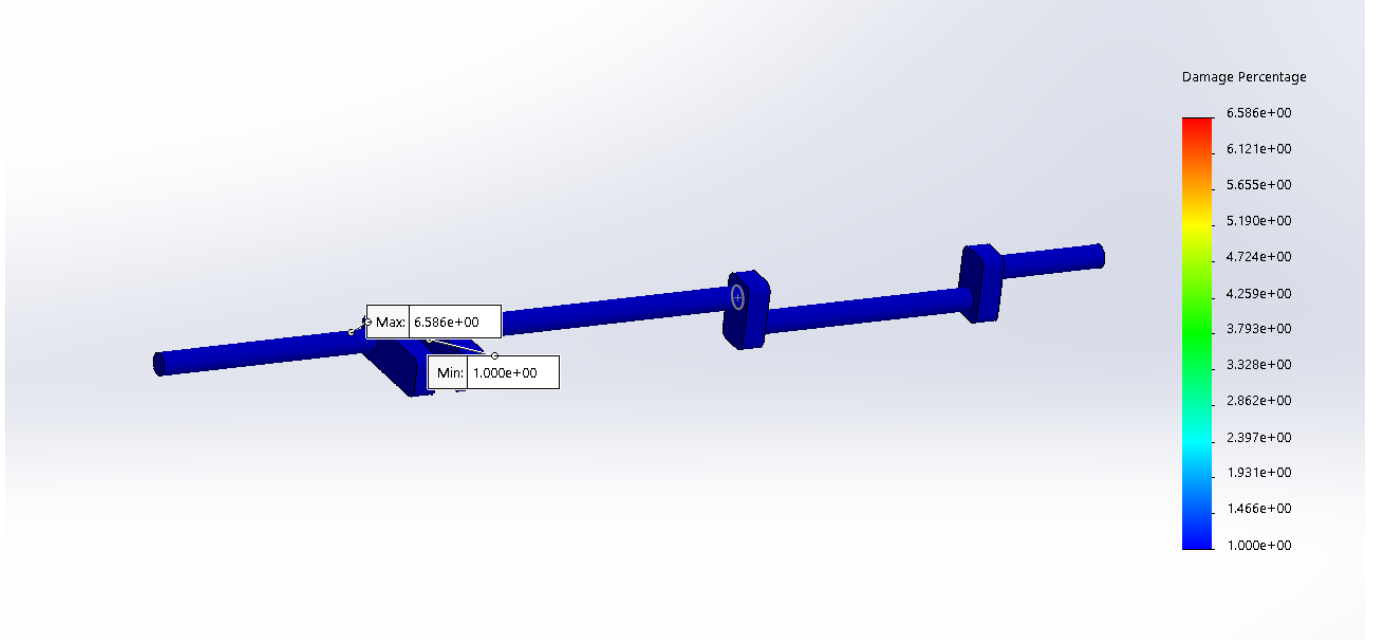


Figure 5.3: Fatigue analysis of crankshaft

5.1.3 Stress and Fatigue Analysis of Displacer

During the engine's operation, the piston head experiences pressures due to combustion. While these pressures vary, they can be approximated using Brake Mean Pressure (BMEP) defined in equation 5.1 [22]. The effective of the BMEP on the displacer and power piston were simulated in Solidworks. Using equation 5.1, the BMEP for the displacer was 5878.4 Pa. This pressure was applied to the displacer, and the results in Figure 5.5 were obtained. With the yield stress being $5.517 \times 10^7 \text{N/m}^2$, the maximum stress experienced was $1.918 \times 10^7 \text{N/m}^2$. Hence, a factor of safety of 2.9 was obtained. In the fatigue test performed, the damage percent after 10,000 cycles was 14.13% as in Figure 5.4.

$$BMEP = \frac{Pn_c}{V_d N} \quad (5.1)$$

Where P = Power Output

n_c = number of revolution per stroke ($n_c = 2$)

V_d = Displacement volume of piston

N = number of revolutions per second

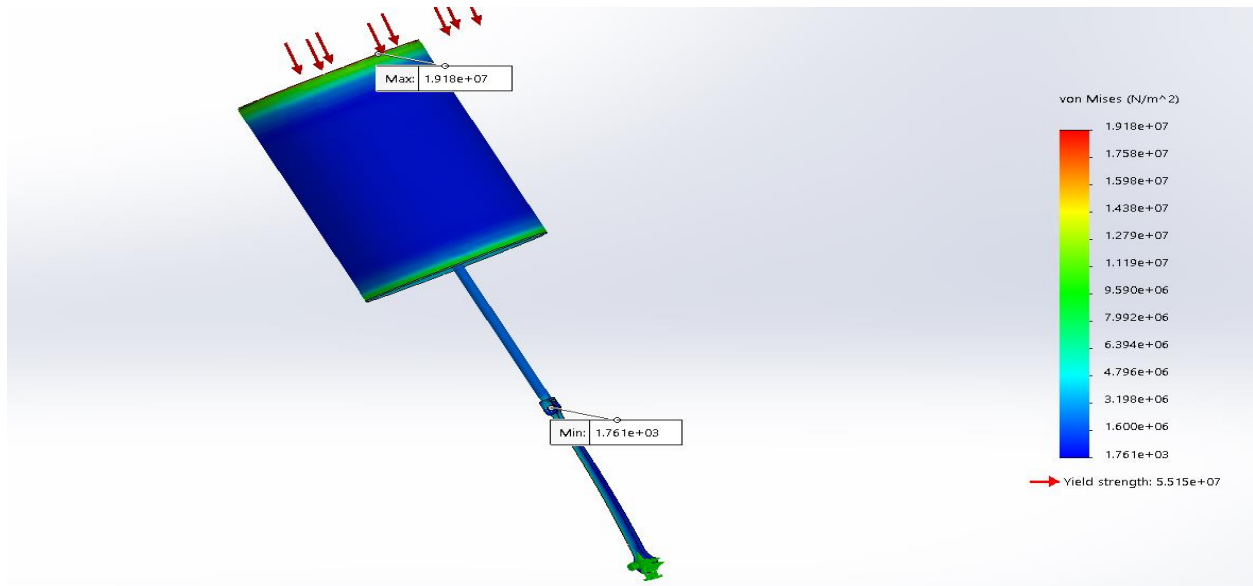


Figure 5.4: Results of the displacer's static analysis

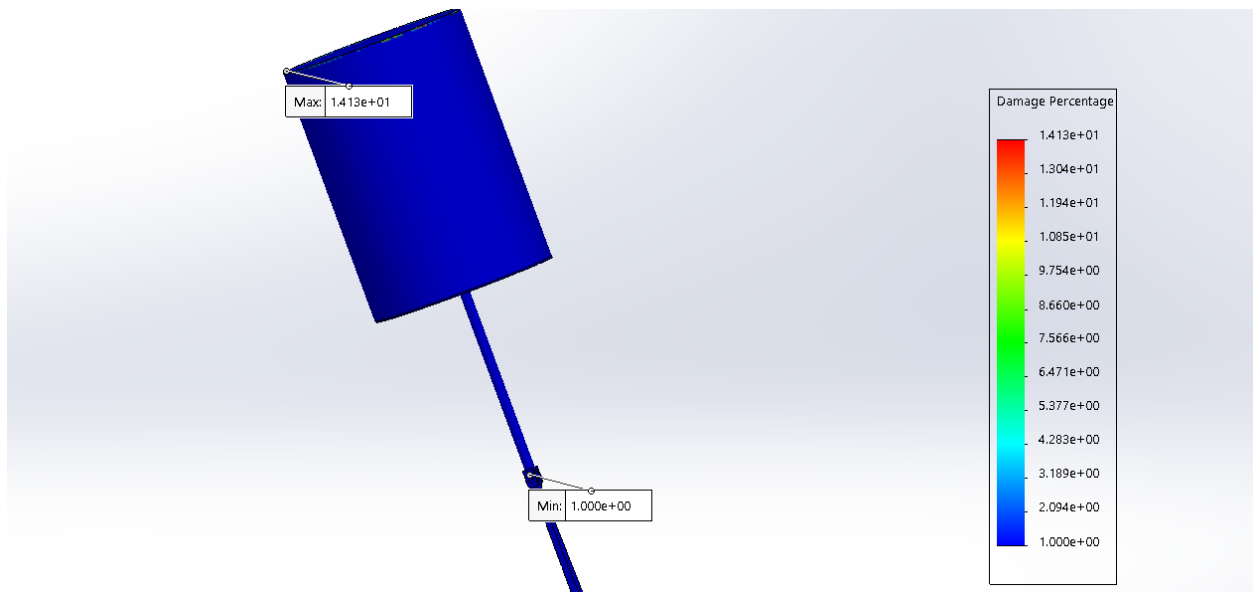


Figure 5.5: Results of the displacer's fatigue analysis

5.1.4 Stress and Fatigue Analysis of Power Piston

Using a BMEP of 47027 Pa, the power piston was also simulated, and the results in Figure 5.7 were obtained. The maximum stress attained was $6.469 \times 10^7 \text{ N/m}^2$, while the yield stress of the material is $2.92 \times 10^8 \text{ N/m}^2$. Therefore, a factor of safety of 4.5 was achieved. The fatigue analysis in Figure 5.6 shows that after a 1000 cycle, the maximum damage percent would be 12.15%.

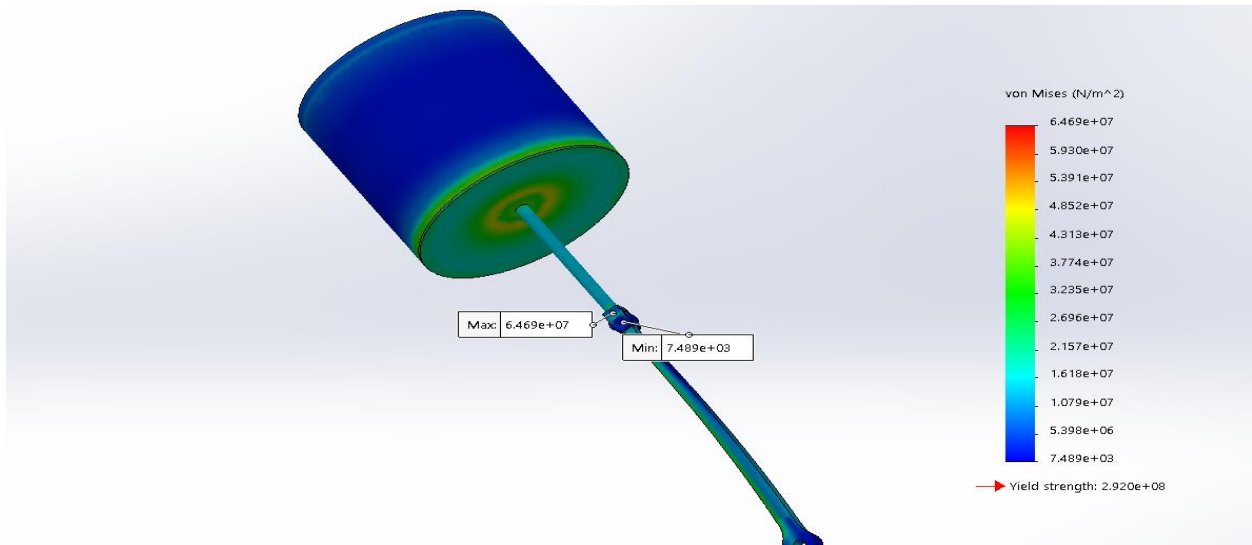


Figure 5.6: Results of power piston's static analysis

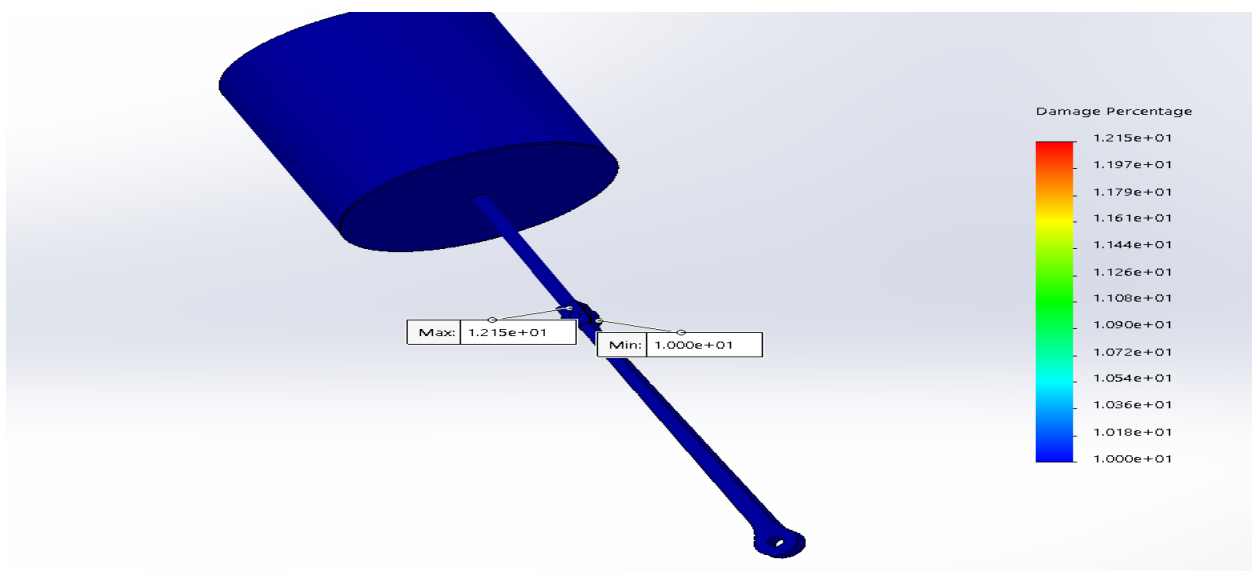


Figure 5.7: Results of power piston's fatigue analysis

5.2 Thermodynamic Analysis

The diagram in Figure 5.8 shows the PV diagram of the designed Stirling engine. From the graph, the net work done was 28.4338 J, which leads to a power output of 568.6752 W. Overall, an efficiency of 19.15 % was achieved. Schmidt analysis was employed to obtain these values. The equations used in the analysis is stated in Appendix B: Schmidt Analysis. The power output obtained is adequate to run an average water pump as the one in Figure 4.1 which needs a power of at least 370 W to work effectively.

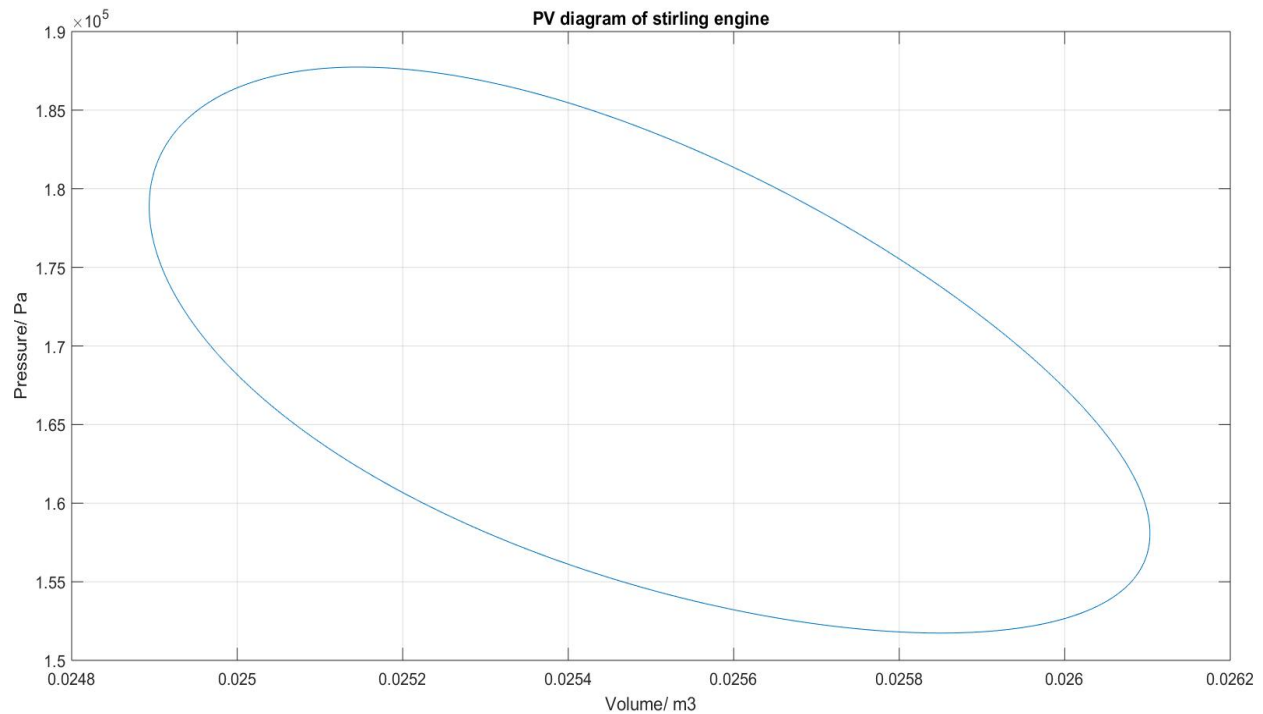


Figure 5.8: PV diagram of Stirling engine

6 Conclusion

This project proves that there is hope for the development of clean and relatively cheap energy for water pumping in rural areas with abundant sunshine. In this engine, concentrated solar energy can be used to heat the hot end of the solar engine to a temperature of 300 °C. Unlike the PV solar system, this system has a relatively cheaper investment cost, and it has a very low carbon footprint [16]. Adopting this technology would lead to the attainment of the SDG 7, to “increase substantially the share of renewable energy in the global energy mix” [5] as stated in chapter 1. Further modifications can be done to the solar-powered Stirling engine to optimize its performance and adapt them for other uses such as electricity generation or any device that requires mechanical energy. Some of these modifications are stated in section 6.2.

6.1 Limitations

The challenges that hindered the accomplishment of the set goals are as follows:

1. Even though the Gamma Stirling engine might be easy to build, it is difficult to get the engine working. This is mainly due to the friction experienced between the crankshaft and the connecting rods. Also, to operate the Stirling engine, the cylinders must be airtight. However, it is extremely difficult to obtain an airtight cylinder.
2. Even though the manufacturing of the Stirling engine using locally outsourced materials might be relatively cheap, the recommended source of heat, that is, Concentrated Solar Power leads to an additional installation cost. However, the system can be scaled such that the engine can be powered by other cheaper heat sources.

6.2 Future Work

This project sets a foundation for the use the Stirling engine technology in areas such as Accra, Ghana. However, other designs and systems can be created to improve upon the work discussed and optimize the use of the Stirling engine. This can be done through the following:

1. Designing a starting mechanism for the Stirling engine such that it does not need an initial push to get it working.
2. Designing and Fabricating a Concentrated Solar Powered Dish to power the Stirling water pump.
3. Fabrication of a thermal storage system such that the Stirling engine can function effectively at night.
4. Designing a more efficient and high-power Stirling engine that can power other devices simultaneously. This would reduce the pressure on the national grid drastically and promote the use of clean energy, thereby protecting the environment.

References

- [1] "Access to electricity (% of population)," [Online]. Available: <https://data.worldbank.org/indicator/eg.Elc.Accs.Zs>.
- [2] N. Patel, "Figure of the week: Electricity access in Africa," 29 March 2019. [Online]. Available: <https://www.brookings.edu/blog/africa-in-focus/2019/03/29/figure-of-the-week-electricity-access-in-africa/>.
- [3] "Global Warming," [Online]. Available: <https://timeforchange.org/what-is-a-carbon-footprint-definition?page=1>.
- [4] "FAQs: Global Poverty Line Update," The World Bank, September 30 2015. [Online]. Available: <https://www.worldbank.org/en/topic/poverty/brief/global-poverty-line-faq>. [Accessed 11 January 2020].
- [5] "Sustainable Development Goal 7," [Online]. Available: <https://sustainabledevelopment.un.org/sdg7#targets>.
- [6] Y. A. Cengel, J. M. Cimbala and R. H. Turner, Fundamentals of Thermal-Fluid Sciences, New York: McGraw-Hill Education, 2017.
- [7] S. M. H. W. Dawi, M. M. Othman, I. Musirin, A. A. M. Kamaruzaman, A. M. Arriffin and N. A. Salim, "Gamma Stirling Engine for a Small Design of Renewable Resource Model," *Indonesian Journal of Electrical Engineering and Computer Science*, vol. 8, no. 2, pp. 350-359, 2017.

- [8] B. Benny, "Seminar Report on Solar Stirling Engine," Kottayam, 2012.
- [9] C. S. Vineeth, *Stirling Engines: A Beginners Guide*, 2011.
- [10] R. K. Bumataria, "Review of Stirling Engines for Pumping Water using Solar Energy as a source of Power," *International Journal of Bioinformatics Research and Applications*, vol. 3, no. 1, pp. 864-868, February 2013.
- [11] M. McHugh, "Solar Powered Stirling Engine," 2017.
- [12] R. Vasu and F. B. Ismail, "Design and implementation of solar powered stirling engines: Review," *AIP Conference Proceedings*, vol. 2035, no. 1, 2018.
- [13] M. He and S. Sanders, "Design of a 2.5kW Low Temperature Stirling Engine for Distributed Solar Thermal Generation," *9th Annual International Energy Conversion Engineering Conference*, p. 5508, 3 August 2011.
- [14] R. Alejandro, "Stirling engine operating at low temperature difference," *American Journal of Physics*, vol. 88, no. 4, pp. 319-324, 2020.
- [15] A. Aditya, G. Balaji, B. Chengappa , K. K. Chethan and S. A. Mohankrishna, "Design and development of Solar Stirling Engine for power generation," *IOP Conference Series: Materials Science and Engineering*, vol. 376, no. 1, June 2018.
- [16] M. Ardon, "Sunvention Sunpulse Water - Solar Thermal Pump," 2010.
- [17] A. Saini, S. Kohli and A. J. Pillai, "Solar powered Stirling engine driven water pump," 2016.

- [18] R. K. Bumataria and N. K. Patel, "Review of Stirling Engines for Pumping Water using Solar as source of Power," *International Journal of Engineering Research and Applications (IJERA)*, vol. 3, no. 1, pp. 864-868, 2013.
- [19] S. M. Wazed, B. R. Hughes, D. O'Connor and J. K. Calautit, "Solar Driven Irrigation Systems for Remote Rural Farms," *Energy Procedia*, vol. 142, pp. 184-191, 2017.
- [20] A. Asnaghi, S. M. Ladjevardi, P. S. Izadkhast and A. H. Kashani, "Thermodynamics Performance Analysis of Solar Stirling Engines," *ISRN Renewable Energy*, vol. 2012, 2012.
- [21] G. Q. Chaudhary, R. Kousar, M. Ali, M. Amar, K. P. Amber, S. K. Lodhi, M. R. u. Din and A. Ditta, "Small-Sized Parabolic Trough Collector System for Solar Dehumidification Application: Design, Development, and Potential Assessment," *International Journal of Photoenergy*, 21 February 2018.
- [22] J. Carvill, "Applied Mechanics," in *Mechanical Engineer's Data Handbook*, Butterworth-Heinemann, 1993, pp. 56-101.
- [23] M. Byl, "Stirling Engine," 2002.
- [24] A. Bar-Cohen and W. M. Rohsenow, "Thermally Optimum Spacing of Vertical, Natural Convection Cooled, Parallel Plates," *Journal of heat Transfer*, vol. 106, pp. 116-123, 1984.
- [25] B. Fid, A. J. Kolios, A. Sowale, A. Parker, T. Somorin, L. Williams, S. Tyrrel, E. McAdam and C. Matt, "Thermodynamic analysis of a gamma type Stirling engine in an energy," *Energy Conversion and Management*, vol. 165, pp. 528-540, 1 June 2018.

- [26] W. R. Martini, *Stirling Engine Design Manual*, Richland, Washington: University of Washington, 1978.
- [27] I. Tlili, Y. Timoumi and S. B. Nasrallah, "Analysis and design consideration of mean temperature differential Stirling engine for solar application," *Renewable Energy*, vol. 33, no. 8, pp. 1911-1921, 2008.
- [28] R. Gheith, F. Aloui and S. B. Nasrallah, "Determination of adequate regenerator for a Gamma-type Stirling," *Applied Energy*, vol. 139, pp. 272-280, 2015.
- [29] M. E. Hofacker, J. Kong and E. J. Barth, "A Lumped-Parameter Dynamic Model of a Thermal Regenerator for Free-Piston Stirling Engines," *ASME 2009 Dynamic Systems and Control Conference*, vol. 1, pp. 237-244, 2009.

Appendix

Appendix A: Modelled and Fabricated Stirling Engine

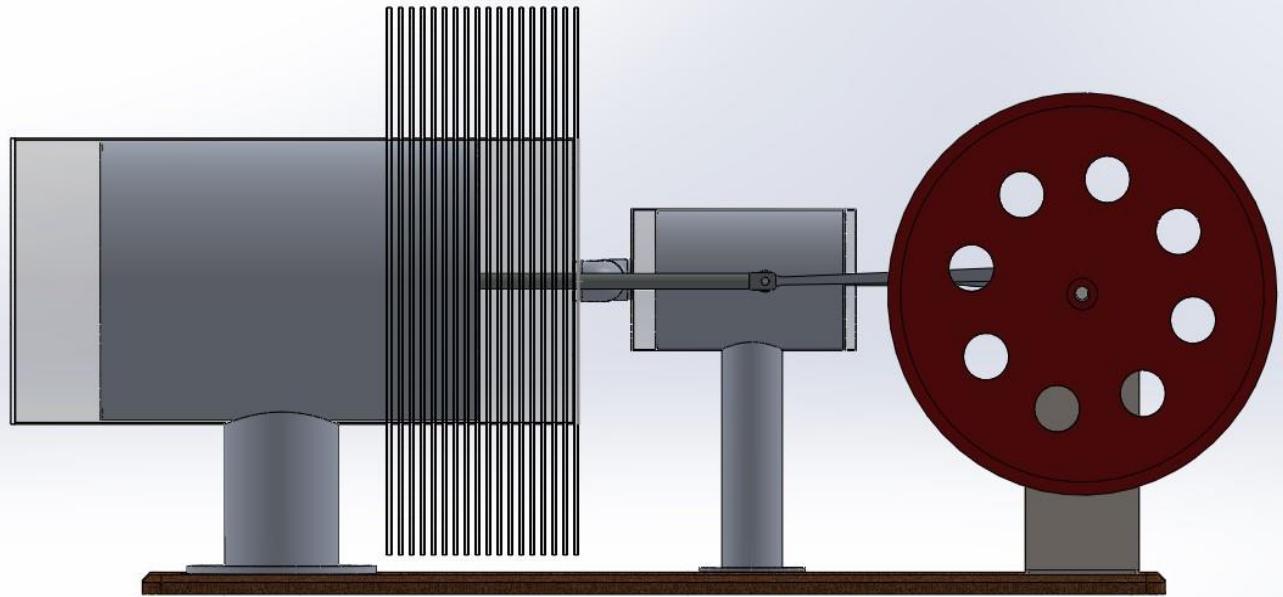


Figure A2: Aside view of designed Stirling Engine

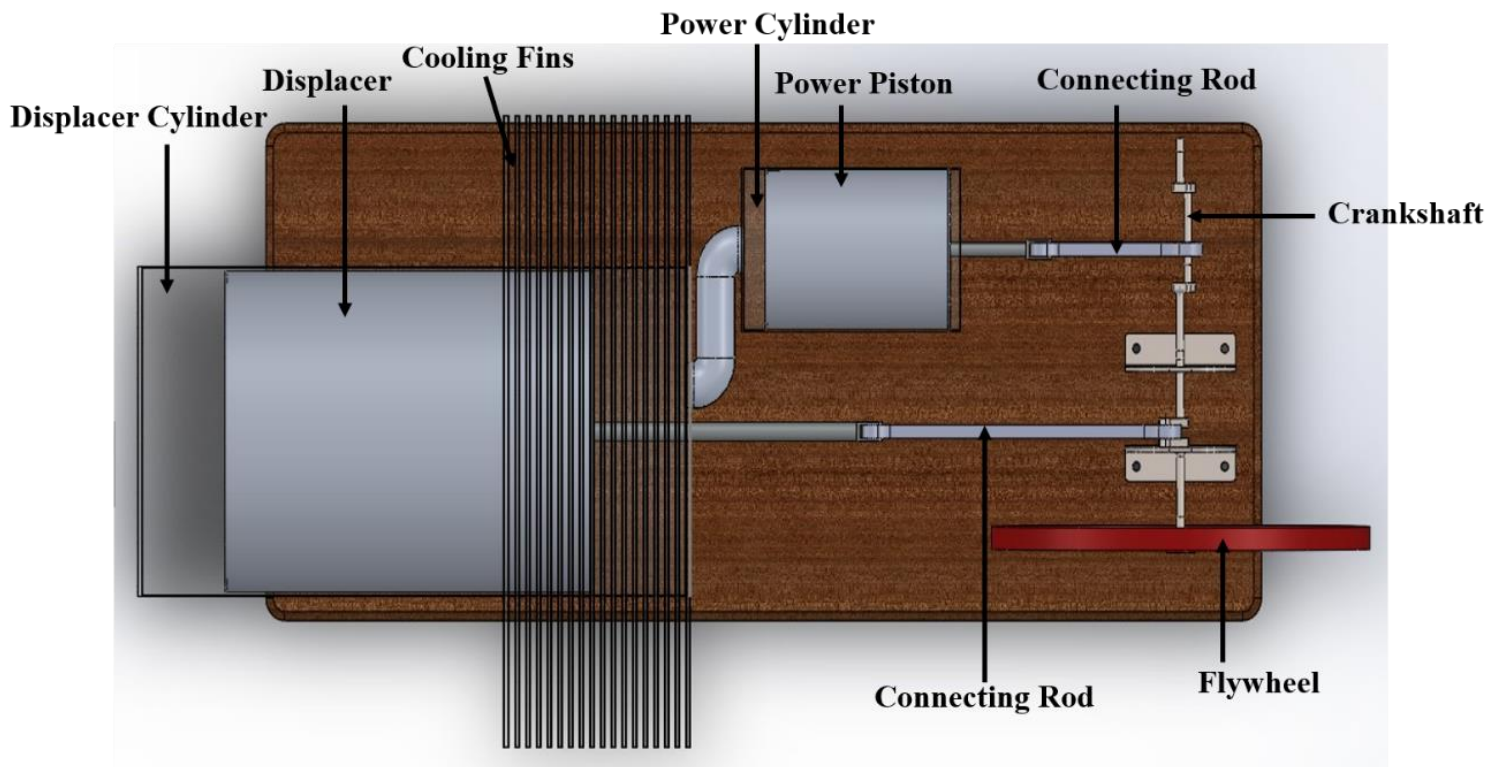


Figure A1 : A top view of designed Stirling engine

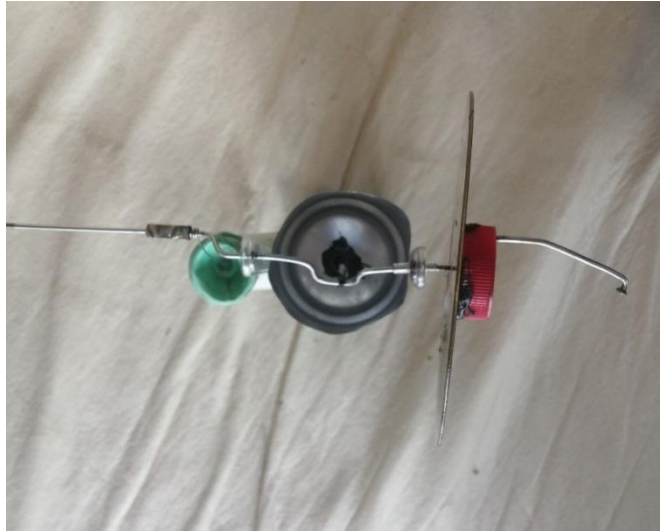


Figure A3:Top view of the prototype built

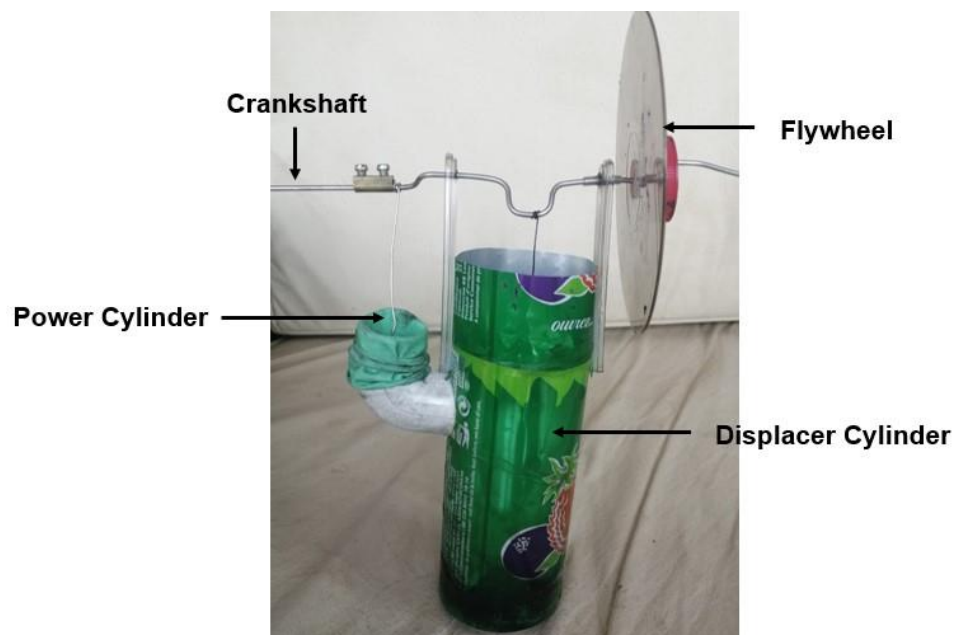


Figure A4:Front view of the prototype built

Appendix B: Schmidt Analysis

Nomenclature for Analysis

Table A 1: Nomenclature for Schmidt Analysis

Variable	Definition and unit
V_{SE}	Swept Volume of displacer piston, m ³
S_{dp}	Displacement of displacer piston, m
B_{dp}	Bore of displacement piston, m
V_{SC}	Swept Volume of power piston, m ³
B_{pp}	Bore of power piston, m
S_{pp}	Displacement of power piston, m
V_E	Expansion space volume
V_C	Compression space volume
ϕ	Phase angle, °
V	Total volume
V_D	Total dead volume
V_{DE}	Dead expansion volume
V_R	Regenerator volume
V_{DC}	Dead compression volume
T_R	Regenerator temperature
T_E	Expansion space temperature
T_C	Compression space temperature
m	Total mass of air
m_E	Mass of air in expansion space
m_R	Mass of air in regenerator space
m_C	Mass of air in compression space
p	Pressure of engine
R	Gas constant of air
W_{net}	Net work done by engine
ω	Speed of engine
P_{output}	Power output of engine
α	Crank angle, °

Assumptions to perform Schmidt Analysis [7], [25]

1. The working gas, which is air in this case, is an ideal gas.
2. The speed and pressure are constant throughout the cycle.
3. The Stirling engine is in steady-state operation
4. There is no leakage of the working gas.
5. The temperature of the working gas changes with time.
6. The regenerator temperature is equal to the average temperatures of the expansion space and compression space temperature.
7. There is a sinusoidal motion between the displacer and the power piston.

Schmidt Analysis [7], [26]

The swept volume of the displacer and power piston was calculated using equation 1 and 2, respectively.

$$V_{SE} = \frac{\pi}{4} \times (B_{dp})^2 \times S_{dp} \quad (1)$$

$$V_{SC} = \frac{\pi}{4} \times (B_{pp})^2 \times S_{pp} \quad (2)$$

The expansion volume is calculated in equation 3. The compression volume, the volume between the displacer and the power piston, is represented in equation 4. Both the expansion and compression volumes are a function of the crank angle. Depending on the point in the cycle, the crank angle is between 0° and 360° .

$$V_E(\alpha) = \frac{V_{SE}}{2} \cdot (1 - \cos \alpha) \quad (3)$$

$$V_C(\alpha) = \frac{V_{SE}}{2} \cdot (1 + \cos \alpha) + \frac{V_{SC}}{2} \cdot (1 - \cos(\alpha - \varphi)) \quad (4)$$

$$\alpha = 0^\circ \text{ to } 360^\circ \quad (5)$$

$$\varphi = 90^\circ \quad (6)$$

The total volume of the cylinder represented in equation 7 comprises of the expansion space volume, the compression space volume and the total dead volume. The total dead volume is the sum of the dead volume in expansion space and compression space and the volume of the regenerator space as represented in equation 8.

$$V(\alpha) = V_E + V_D + V_C \quad (7)$$

$$V_D = V_{DE} + V_R + V_{DC} \quad (8)$$

The temperature of the regenerator can be determined using equation 9.

$$T_R = \frac{T_E - T_C}{\ln\left(\frac{T_E}{T_C}\right)} \quad (9)$$

The total mass of the working gas, air, comprises of the mass of expansion, regenerator and compression space as expressed in equation 10 and expanded in equation 11.

$$m = m_E + m_R + m_C \quad (10)$$

$$m = \frac{p}{R} \cdot \left[\frac{V_E}{T_E} + \frac{V_R}{T_R} + \frac{V_C}{T_C} \right] \quad (11)$$

Equation 11 is rearranged to obtain the pressure at each point in the cycle, as shown in equation 12.

$$p = \frac{M \times R}{\frac{V_E}{T_E} + \frac{V_R}{T_R} + \frac{V_C}{T_C}} \quad (12)$$

These equations are inserted into MATLAB with their corresponding values. The pressure is plotted against the total volume to obtain the PV diagram in Figure 5.8.

$$Q_s = P_3 V_3 \ln \left(\frac{V_4}{V_3} \right) \quad (13)$$

$$Q_R = P_1 V_1 \ln \left(\frac{V_1}{V_2} \right) \quad (14)$$

$$W_{net} = Q_s - Q_R \quad (15)$$

$$P_{output} = W_{net} \times \omega \quad (16)$$

Where $P_3 = \text{pressure at state 3}$

$P_1 = \text{pressure at state 1}$

$V_3 = \text{volume at state 3}$

$V_1 = \text{volume at state 1}$

These equations are inserted into MATLAB with their corresponding values. The pressure is plotted against the total volume to obtain the PV diagram in Figure 5.8. The values of P_1 , P_3 , V_3 and V_1 were obtained using the PV diagram and inserted into equation 13 and 14 to obtain the net work done in equation 15 by the engine. The power produced by the engine is calculated using equation 16. Finally, the efficiency of the engine is obtained in equation 17.

$$\eta = 1 - \frac{Q_s}{Q_R} \quad (17)$$

Appendix C: Drawings of the Parts of the Stirling Engine

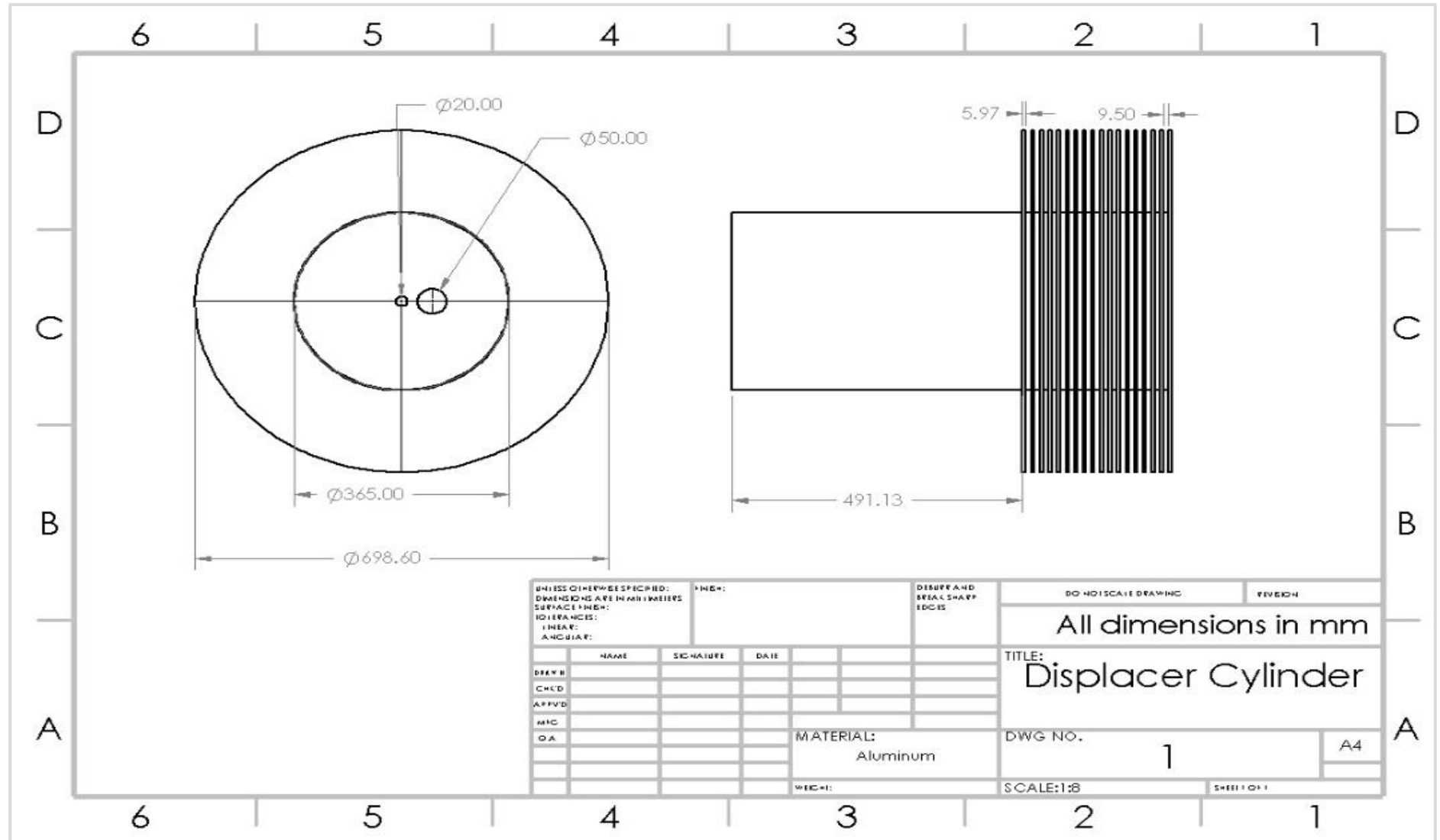


Figure C1: Drawing of Displacer Cylinder

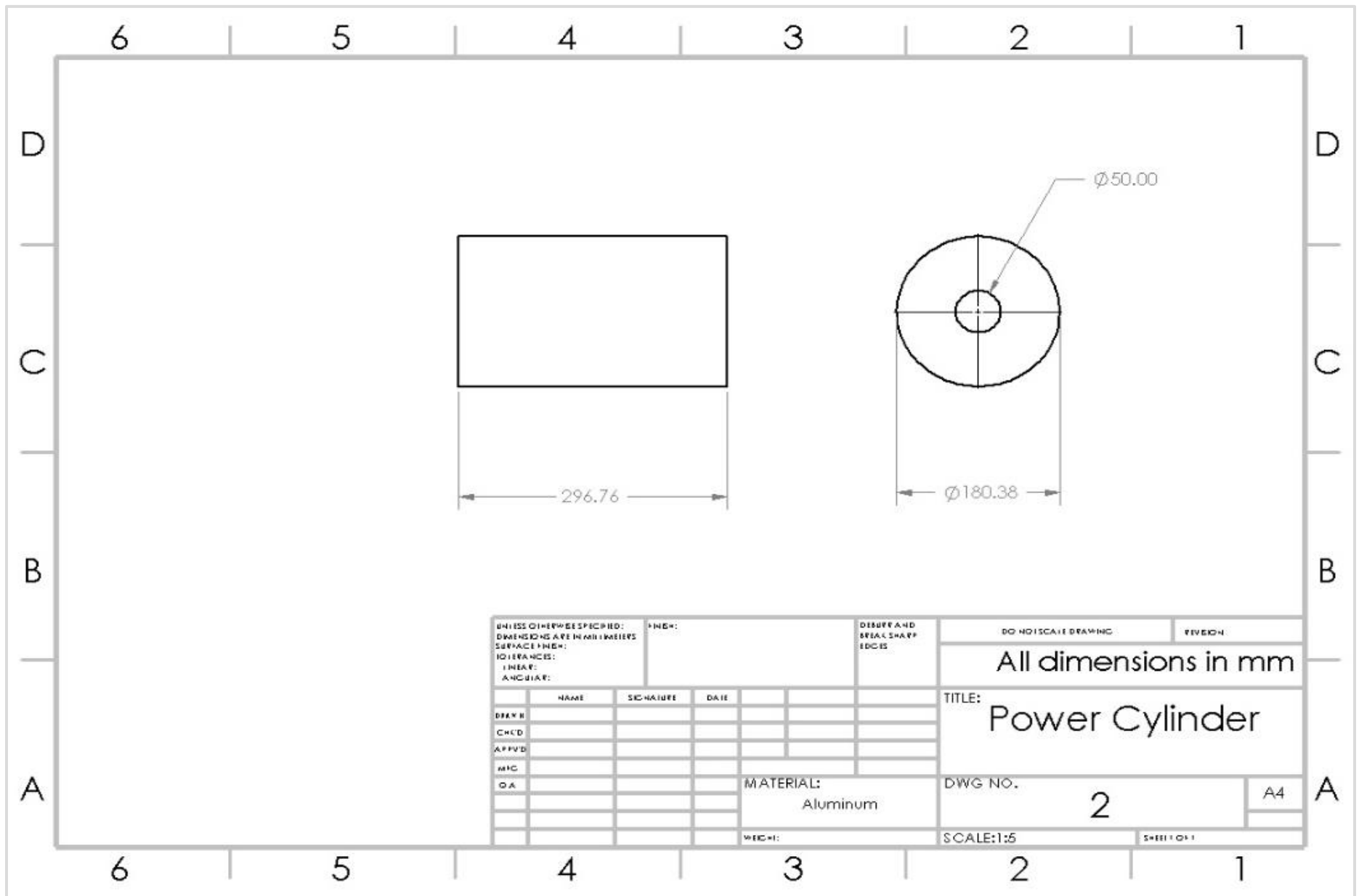


Figure C2: Drawing of Power Cylinder

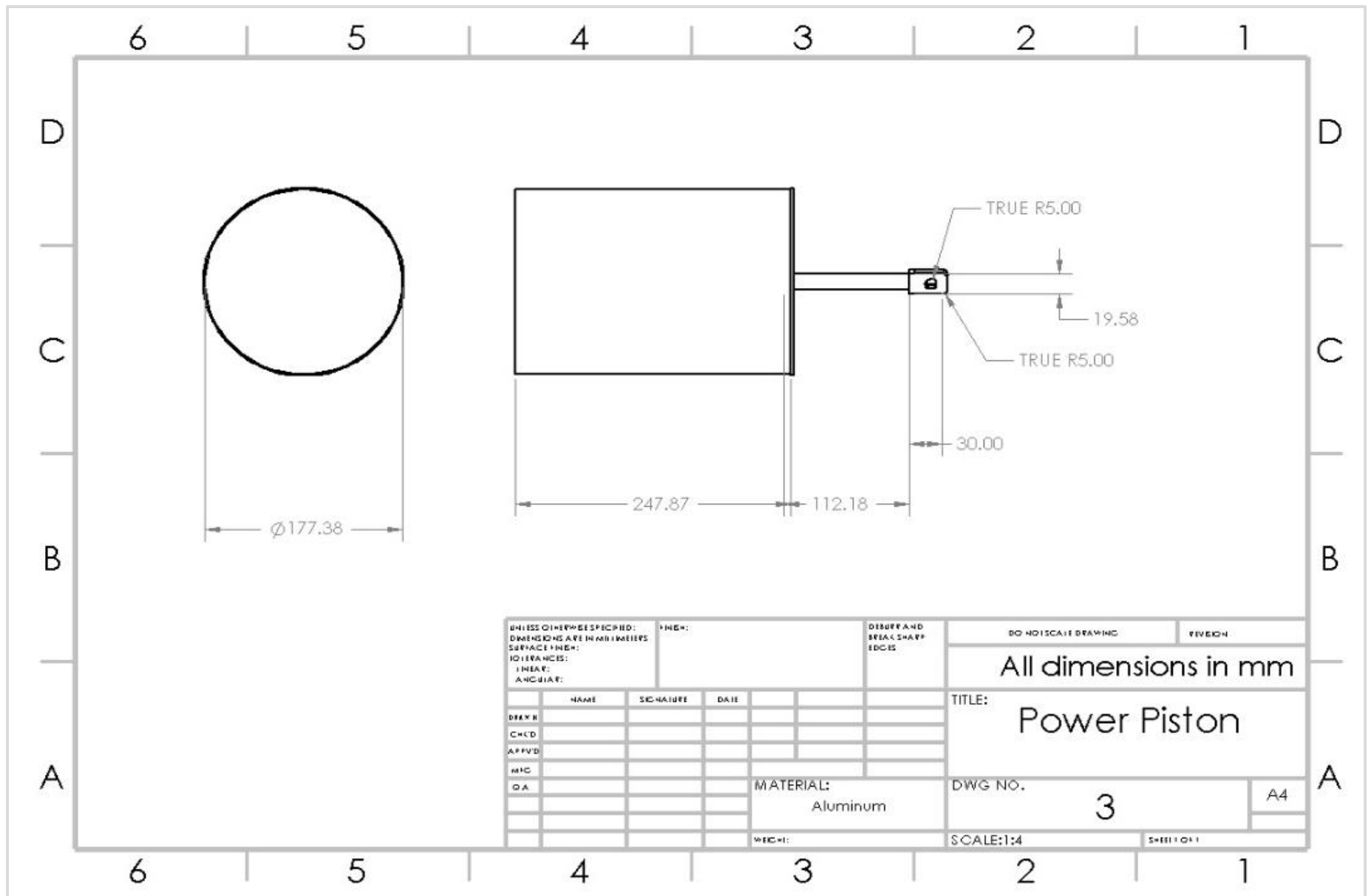


Figure C3: Drawing of Power Piston

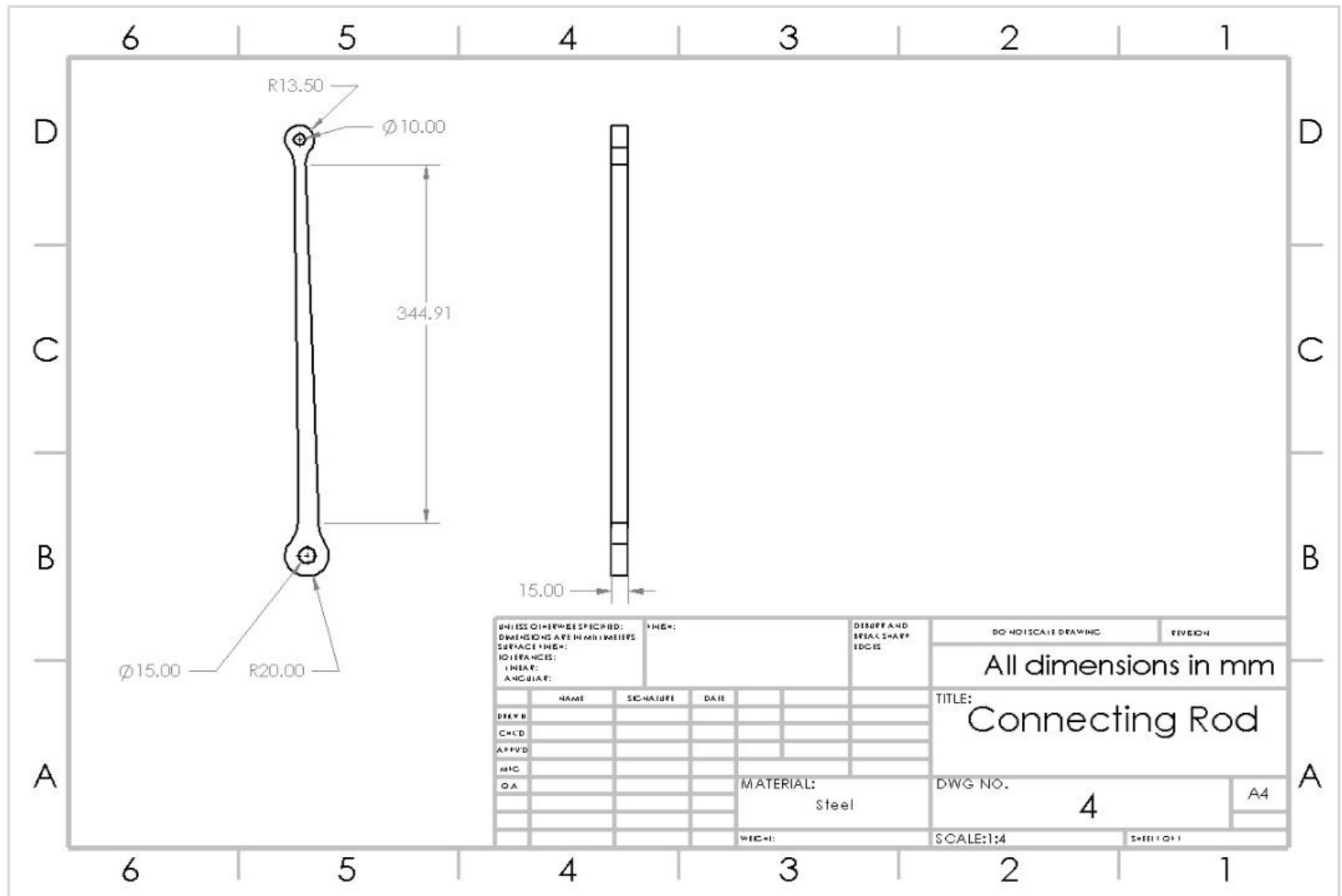


Figure C4: Drawing of Connecting Rod

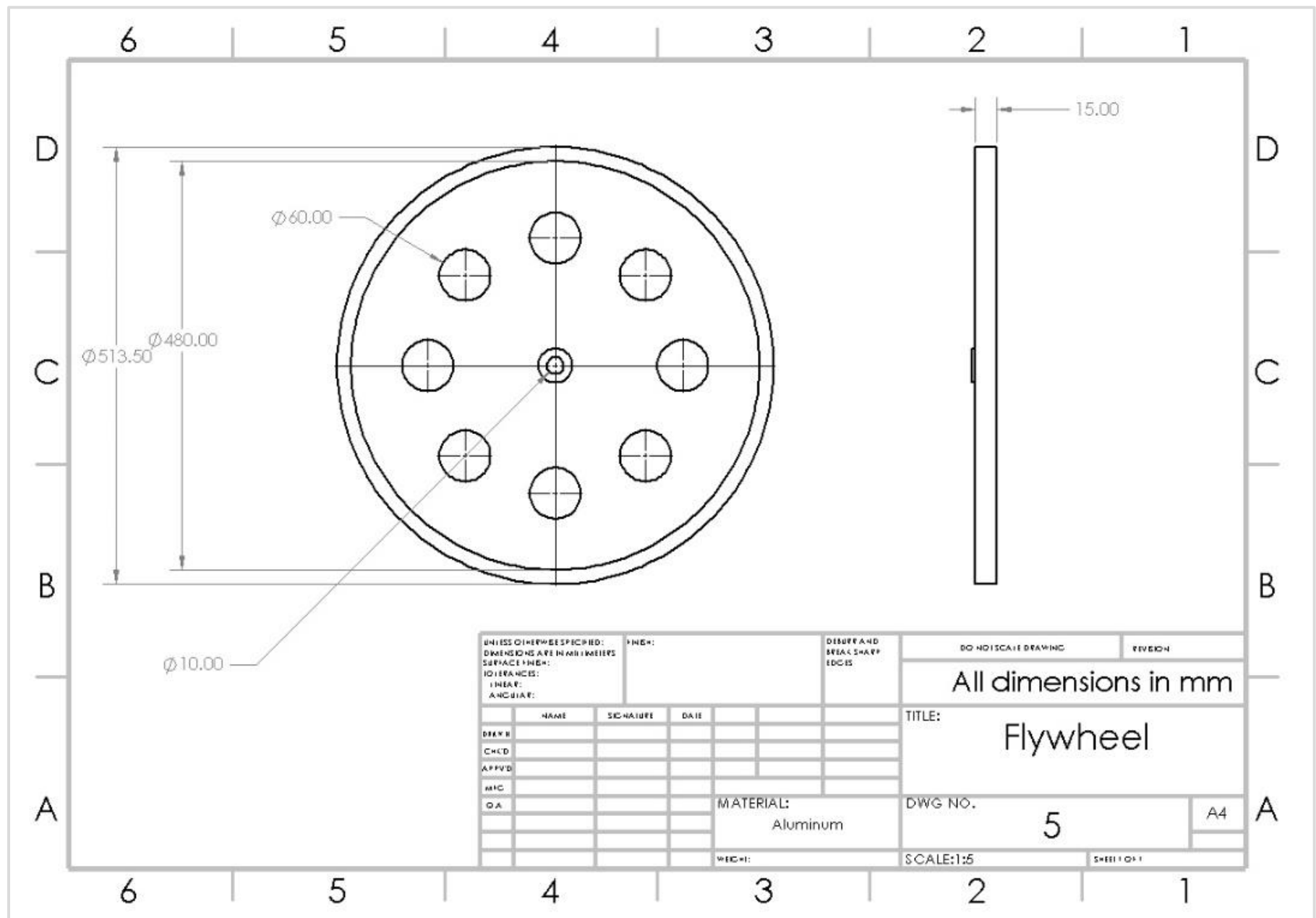


Figure C5: Drawing of Flywheel

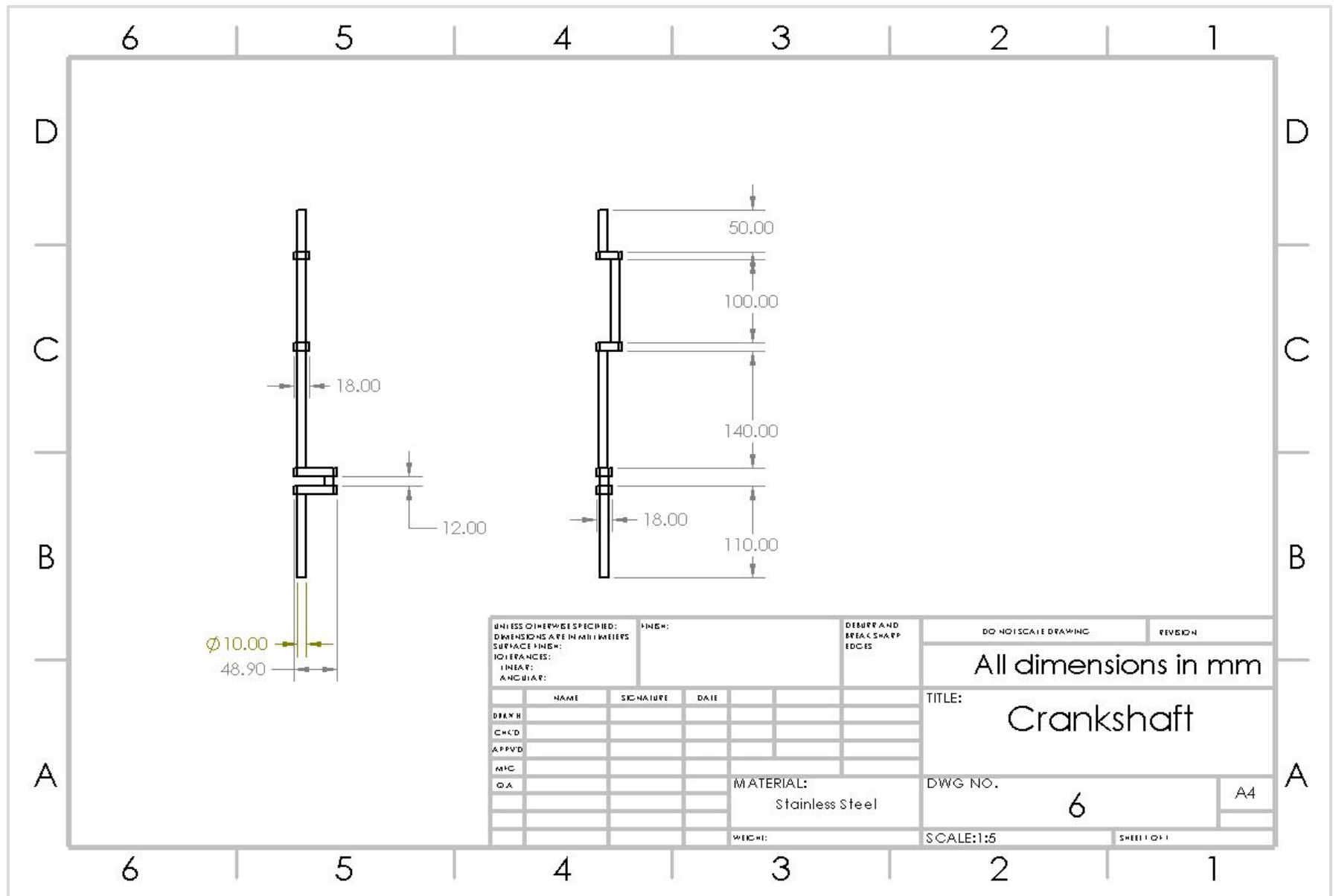


Figure C6: Drawing of Crankshaft

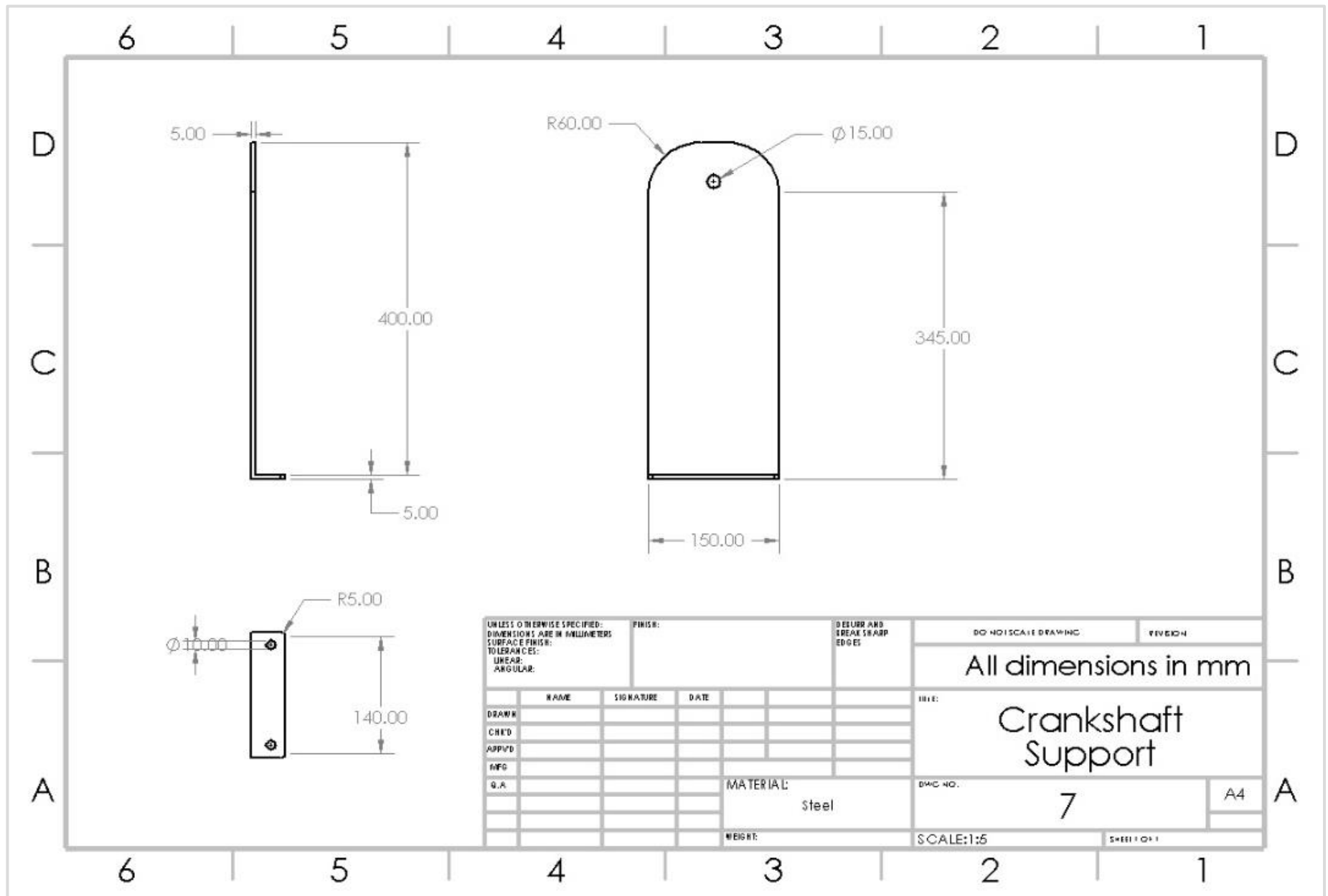


Figure C7: Drawing of Crankshaft Support

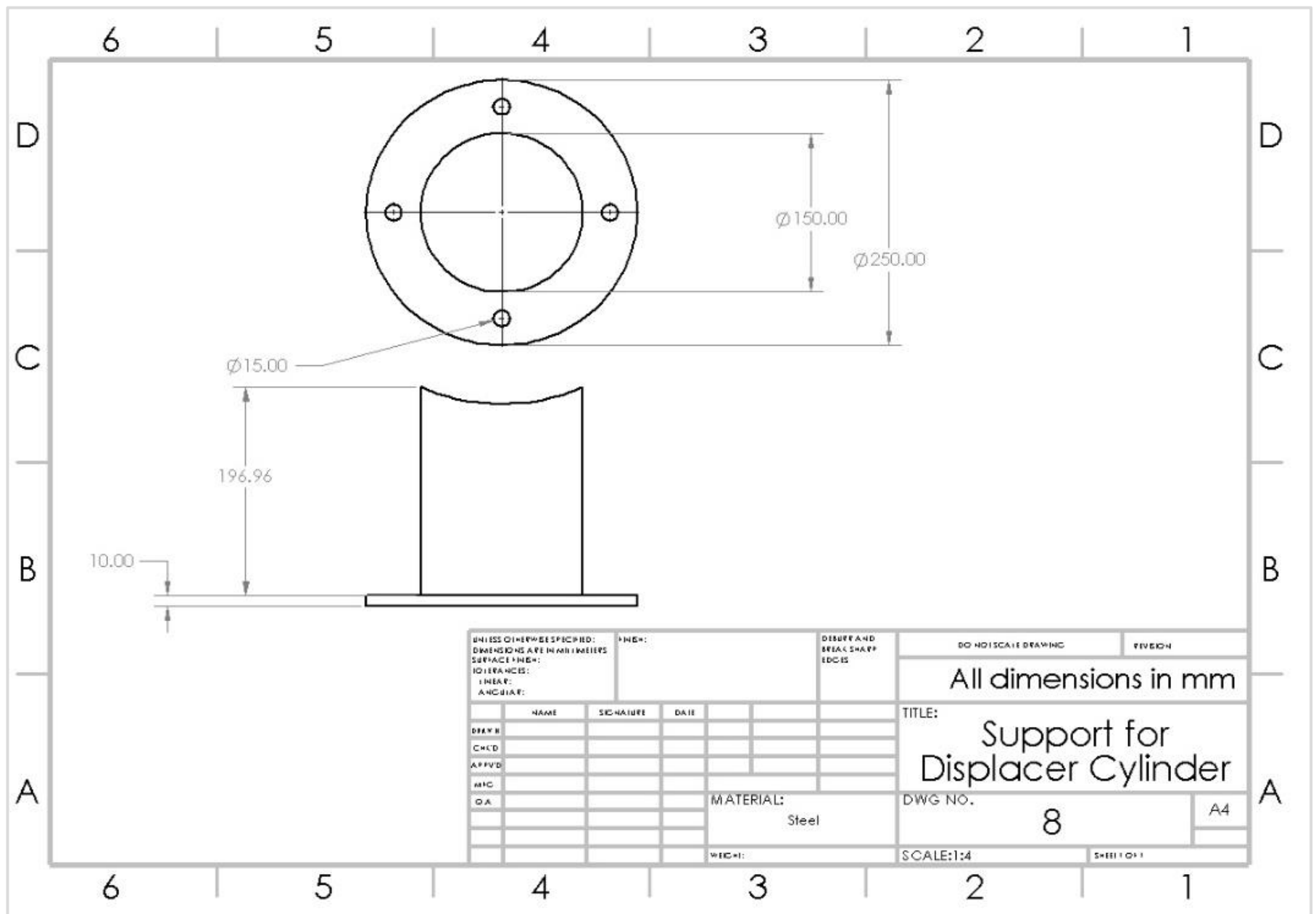


Figure C8: Drawing of the Displacer Cylinder's Support

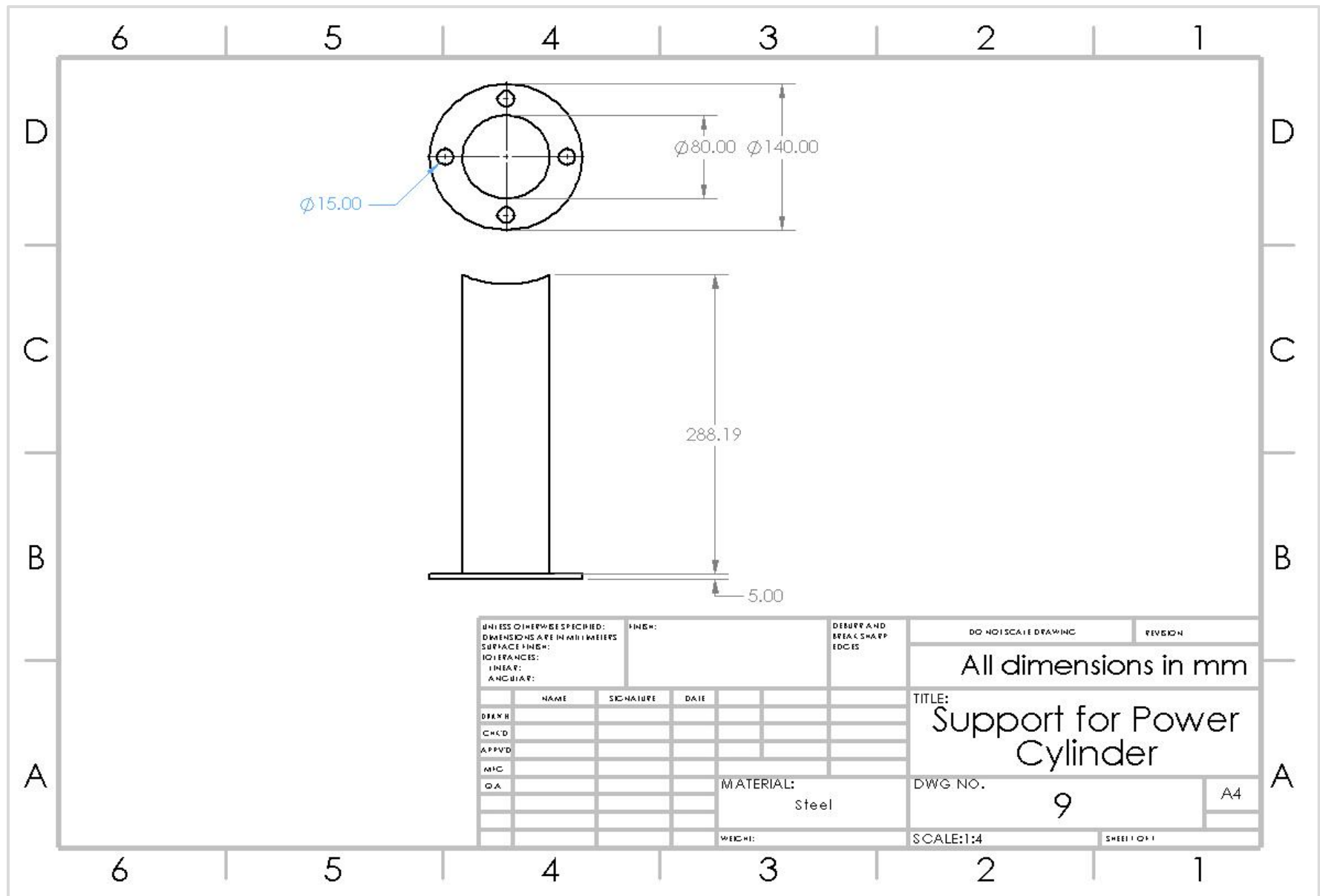


Figure C9: Drawing of Power Cylinder's Support

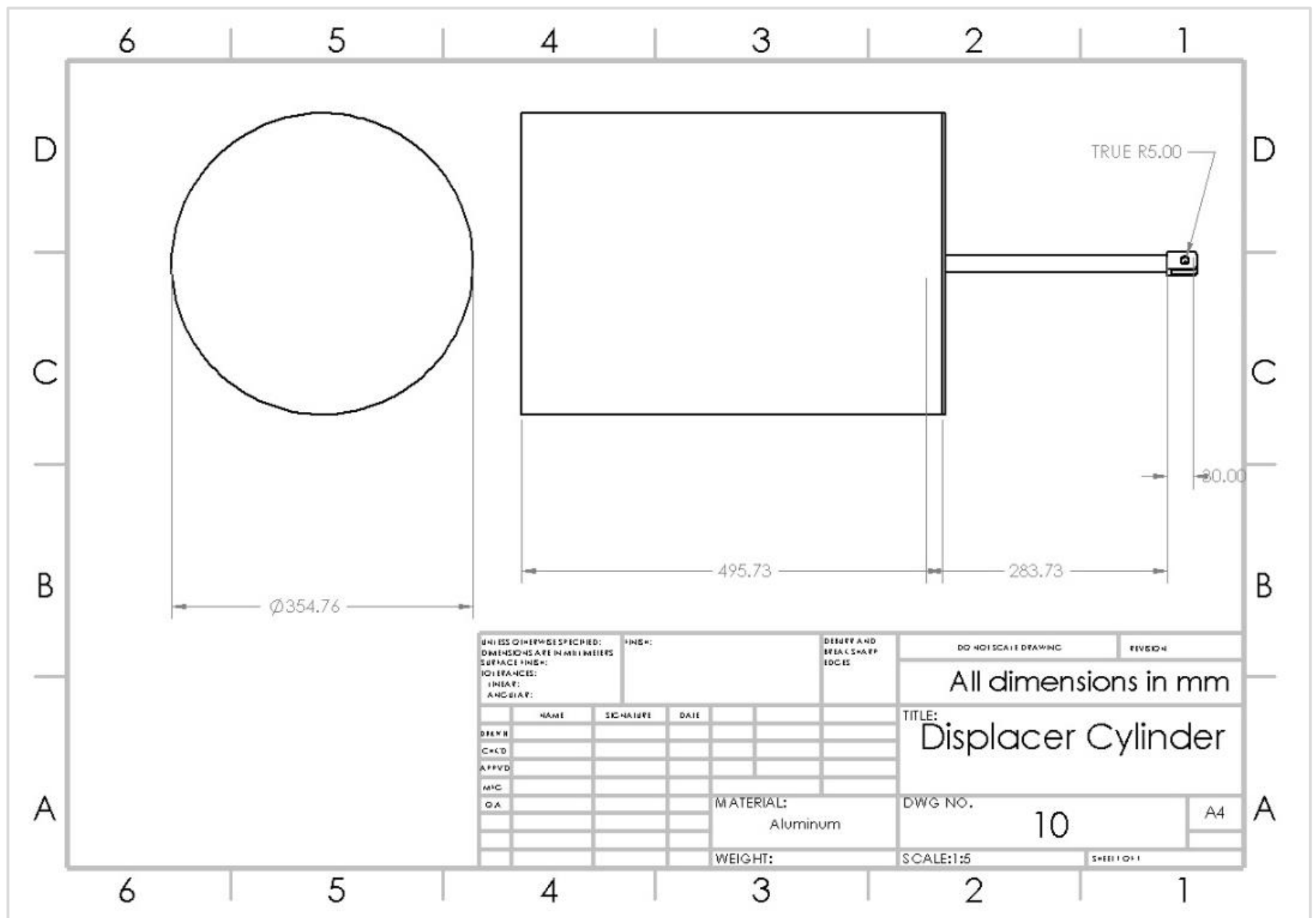


Figure C10: Drawing of Displacer Cylinder

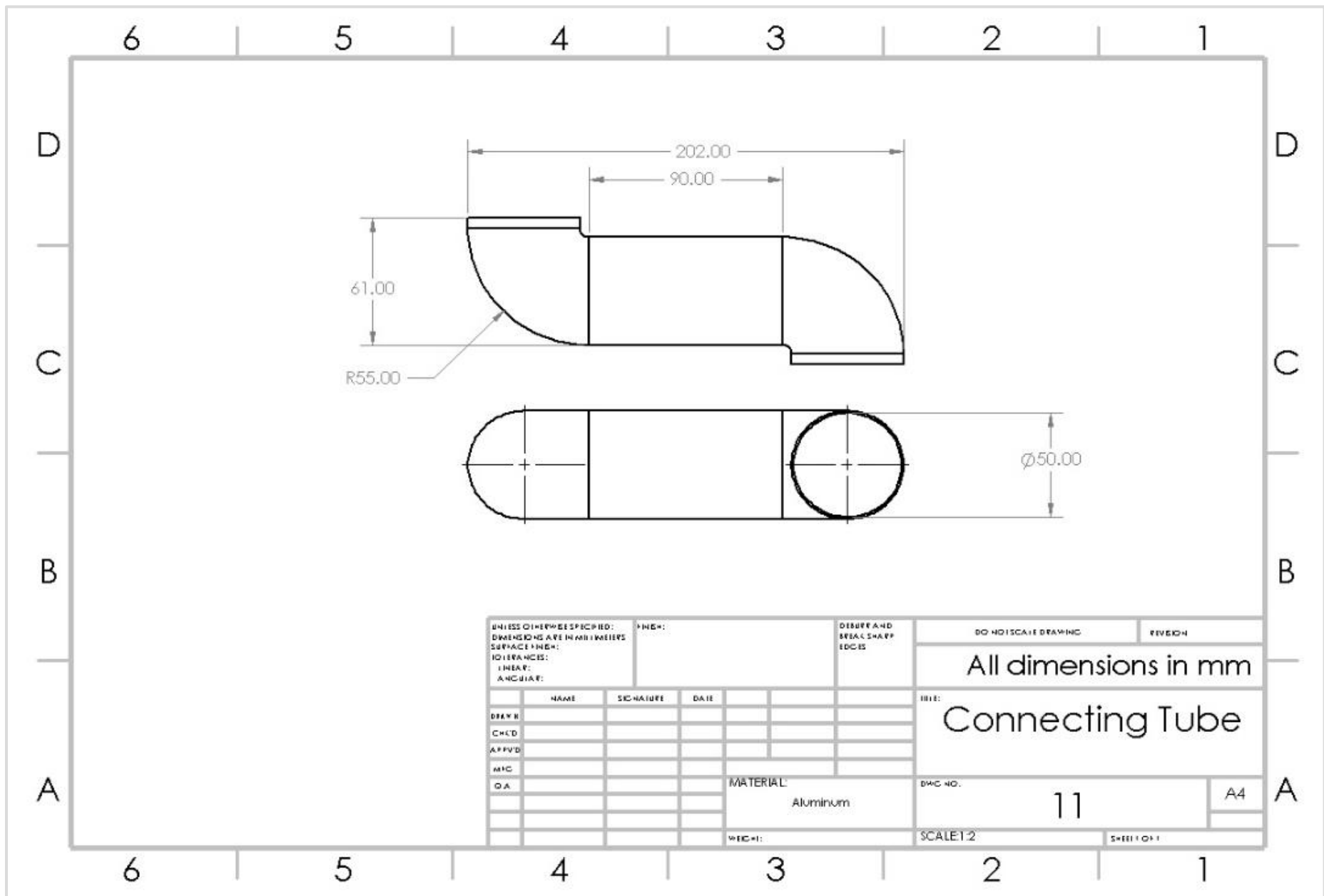


Figure C11: Drawing of Connecting Tube

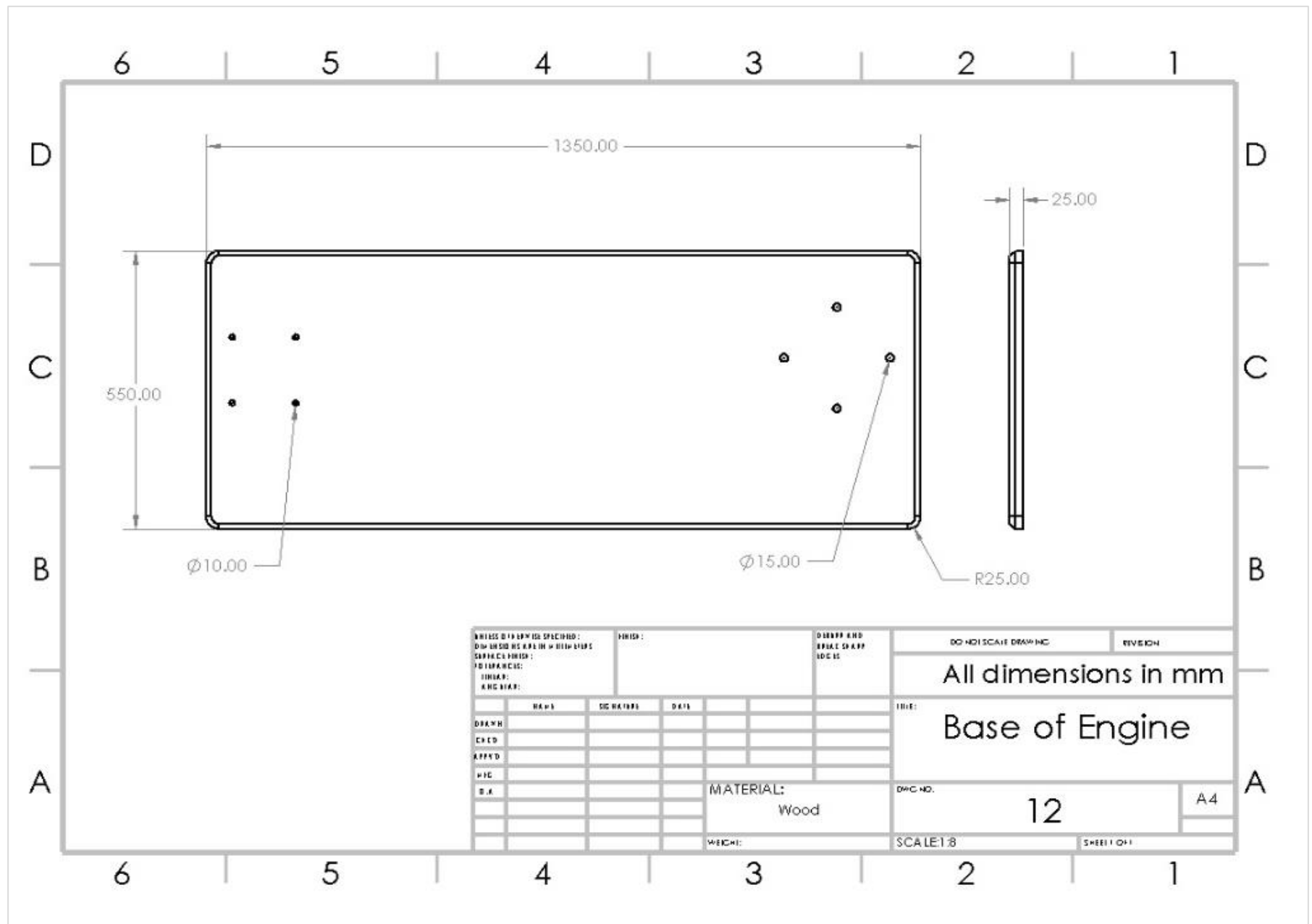


Figure C12: Drawing of the base of the Engine

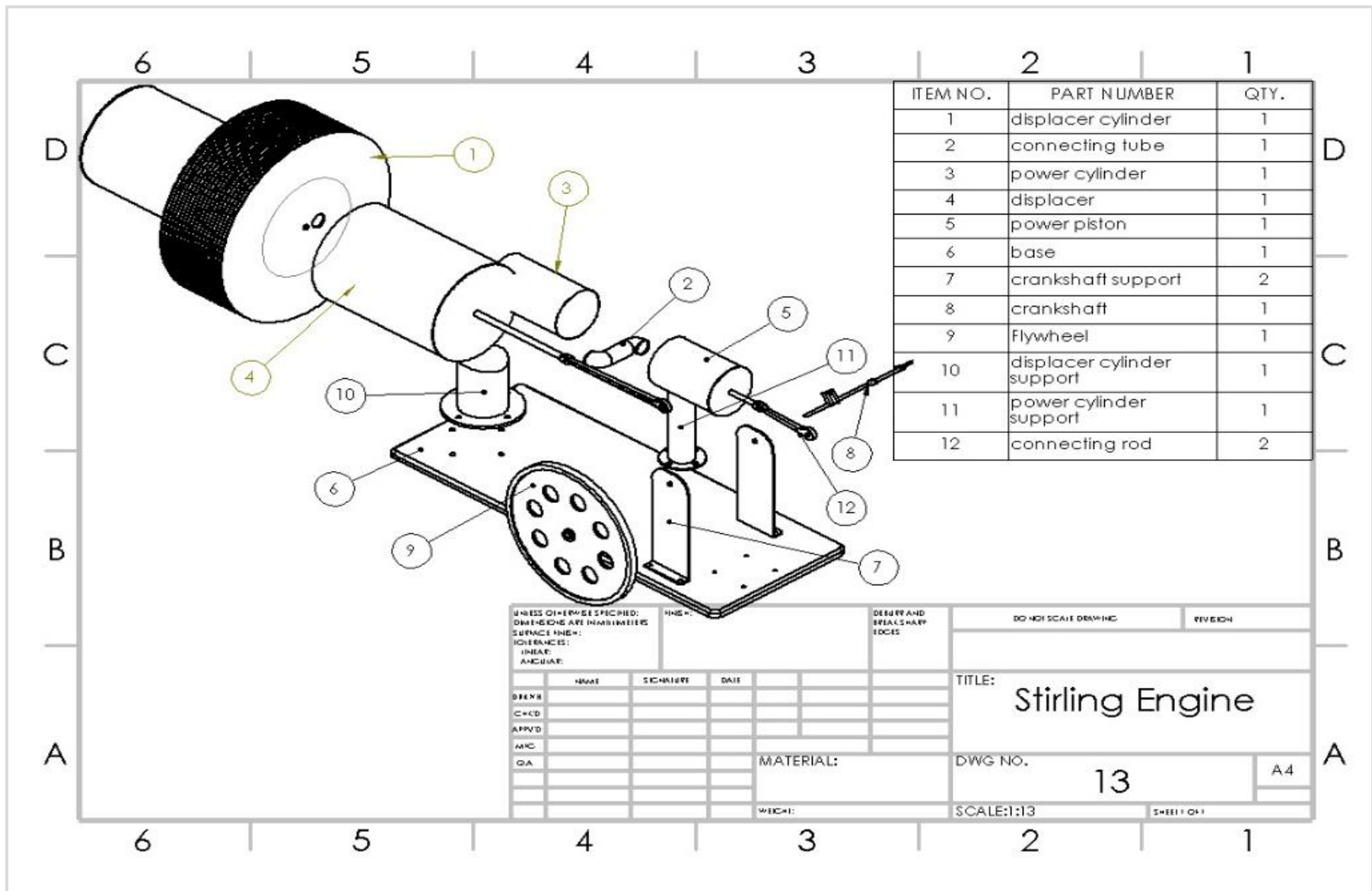


Figure C13: Exploded View of Stirling Engine